Techno-Economic and Dynamic Performance Optimization of a Hybrid PV–Wind–BESS Microgrid for Rural Electrification

B.O. Ariyo[1, 2*], L.M. Adesina[1], O. Ogunbiyi[1], A. Musa[1, 3], B.J. Ojuolape[1], M.O. Balogun[1]

[1]Department of Electrical and Computer Engineering, Faculty of Engineering and Technology, Kwara State University, Malete, Nigeria

[2]Department of Electrical and Electronics Engineering, Faculty of Engineering and Technology, University of Ilorin, Nigeria

[3]Institute for Intelligent Systems, University of Johannesburg, South Africa

ABSTRACT: The escalating global energy demand and reliance on renewables highlight the need for sustainable and reliable power solutions. This study investigates the feasibility of a hybrid PV-Wind-BESS microgrid to provide clean electricity for underserved communities, using Olowo-Oko in Kwara State, Nigeria, as a case study. Average daily loads of 19.72 kWh (rainy season) and 22.95 kWh (dry season) were recorded using a Fluke 432-II Power Analyzer. Solar irradiance and wind speed data were sourced from NASA. The microgrid was modelled and simulated in MATLAB Simulink, incorporating advanced control strategies for voltage and frequency regulation. Techniques such as Triangular and Sinusoidal Pulse Width Modulation (TPWM and SPWM), combined with passive filters, effectively mitigated harmonics and enhanced power quality. Simulation results showed stable dynamic performance, minimal ripple, and efficient renewable integration. Further validation using HOMER Pro enabled techno-economic optimisation, achieving a 96.8% renewable fraction, a levelized cost of energy (LCOE) of $0.033/kWh, and a payback period of 8 years and 10 days. Sensitivity analysis identified battery cost and inverter performance as key factors influencing system viability. The proposed dual mode microgrid, validated through both dynamic modelling and financial simulation, demonstrates technical robustness and economic feasibility for decentralized rural electrification in Sub-Saharan Africa. This integrated framework offers valuable insights for energy developers, researchers, and policymakers aiming to scale up low-carbon, community-based energy systems. By advancing hybrid microgrid modelling, adaptive control techniques, and cost optimization strategies, the study contributes to the practical realization of Sustainable Development Goal (SDG) 7, supporting universal access to affordable, reliable, and clean energy.

KEYWORDS: HOMER Pro Simulation, MATLAB Simulink Modeling, Microgrid (MG) Optimization, Renewable Energy Integration, Rural Electrification, Techno-Economic Analysis.

[Received Dec. 8, 2024; Revised July 7, 2025; Accepted July 18, 2025] Print ISSN: 0189-9546 | Online ISSN: 2437-2110

I. INTRODUCTION

In an era marked by accelerating global population growth and rising industrial demand, access to affordable, reliable, and sustainable electricity remains a critical global challenge (Nur-e-alam et al., 2025; He et al., 2025; Ebrahimi et al., 2021). The world population is projected to reach 8.6 billion by 2030 and 9.8 billion by 2050 (Singh & Gope, 2021), resulting in a steep rise in energy demand, particularly in developing regions where grid infrastructure is often weak or non-existent (Twaisan & Bar, 2022). Empirical data indicate that in such economies, a 1% increase in gross domestic product (GDP) leads to approximately a 1.4% increase in electricity demand (Vaish et al., 2023; Zulu et al., 2023). Meeting this growing demand through conventional fossil-based systems raises serious concerns, including environmental degradation, volatile fuel prices, and energy insecurity (Al-Mahammedi & Onat, 2025; Zadehbagheri et al., 2025).

Microgrid (MG) systems, integrating distributed energy resources (DERs) such as solar photovoltaic (PV), wind turbines (WT), and battery energy storage systems (BESS), offer a promising solution for improving energy reliability, supporting grid resilience, and reducing greenhouse gas emissions (Hernández-Mayoral et al., 2024; Hoarcă et al., 2023). However, the intermittent and variable nature of renewable resources, combined with seasonal and daily variations in load demand, introduces substantial challenges in maintaining voltage and frequency stability, ensuring adequate power quality, and achieving overall system efficiency (Mazorra-Aguiar et al., 2021).

Although prior studies have explored renewable microgrid modeling and optimization, most focus on isolated

*Corresponding author: *mbenghanem@iu.edu.sa*

doi: http://dx.doi.org/10.63746/njtd.v22i5.3158

aspects such as economic analysis, component-level design, or generation optimization. Few studies integrate dynamic control, storage coordination, and real-world load profiles, leaving rural microgrids vulnerable to operational inefficiencies, underutilization of infrastructure, and supply interruptions. This underscores the unresolved problem: the lack of an integrated framework that ensures both technical robustness and economic feasibility for community-specific rural microgrids.

This study develops an optimized dual-mode renewable microgrid system for the Olowo-Oko community, integrating PV, WT, and BESS with advanced inverter and control strategies. Using MATLAB Simulink for dynamic simulations and HOMER Pro for long-term techno-economic optimization, the research provides a comprehensive framework that:

I. Accounts for real-world, seasonally varied load profiles from the Olowo-Oko community;
II. Validates dynamic voltage and frequency stability, along with power quality;
III. Determines optimal system configuration based on capital cost, LCOE, and renewable fraction;
IV. Assesses financial feasibility, including payback period and long-term revenue.

By bridging dynamic operational modeling and long-term economic analysis, this research delivers a practical, scalable, and cost-effective hybrid microgrid solution for rural electrification, advancing the state-of-the-art and addressing critical gaps left by previous studies (Nur-E-Alam et al., 2025).

Several studies have investigated microgrid design, renewable integration, and control strategies. Zehra et al. (2022) and Soudagar et al. (2021) demonstrate that MGs enhance energy reliability and support the grid. However, these works often assume idealized generation conditions and do not account for interactions between renewable variability and storage, limiting their applicability in realistic rural contexts. Ekanayake & Navaratne (2020) and Ejuh Che et al. (2025) highlight voltage and frequency stability challenges arising from renewable intermittency but do not consider integrated dual-mode operation, which is essential for operational robustness in rural microgrids.

Photovoltaic modeling studies (Al-Ezzi & Ansari, 2022; Bilendo et al., 2023; Kareem et al., 2025) provide insights into solar generation under varying insolation and temperature conditions. MPPT techniques such as Perturb and Observe (P&O) have been widely applied to maximize PV output (Ghayth, Yusupov, & Khaleel, 2023; Djilali et al., 2024; Nadzim et al., 2023). While these studies improve PV performance, they often neglect integration with microgrid-level control, storage management, and economic assessment, leaving a gap in practical operational modeling.

Wind energy research reveals turbine output sensitivity to site-specific wind speeds, cut-in, rated, and cut-out thresholds (Letzgus & Müller, 2024; Marti-Puig et al., 2024; Odoi-Yorke & Woenagnon, 2021; Assad et al., 2022; Alam & Jin, 2023). Although the physics of wind energy conversion is well studied, prior work rarely examines coordinated operation with PV and storage in a dual-mode microgrid, limiting insights into realistic system stability and reliability.

Battery storage studies emphasize its role in mitigating renewable intermittency and maintaining energy balance (Bhatti et al., 2024; Andreotti et al., 2024). Yet, many studies simplify battery behavior and fail to connect charge/discharge dynamics with PV, WT, and inverter control, leaving system-wide operational performance underexplored.

Techno-economic analyses, including LCOE, Net Present Cost (NPC), and payback period, are frequently reported (Ekpoh et al., 2025; Kumar et al., 2024; Sawadogo et al., 2025). However, few studies integrate these metrics with dynamic control validation, real load profiles, and multi-resource coordination, limiting the design of microgrids that are both technically robust and financially viable.

Collectively, prior studies indicate that while PV, wind, and battery systems have been individually studied, the following gaps persist:

1) Lack of integrated dual-mode microgrid modeling, combining dynamic stability (voltage/frequency control) with long-term economic optimization;
2) Insufficient use of real community-specific load profiles, particularly for rural applications;
3) Limited assessment of DER coordination, storage management, inverter control, and renewable fraction optimization to ensure practical operational reliability.

This research addresses these gaps by:

- Developing a dual-mode renewable microgrid integrating PV, WT, BESS, and inverter with advanced control;
- Incorporating real field load data from Olowo-Oko, reflecting seasonal and daily variations;
- Optimizing system configuration, renewable fraction, and techno-economic performance, including LCOE and payback period;
- Validating results using both MATLAB Simulink and HOMER Pro, ensuring operational feasibility and real-world applicability.

This work contributes to the growing body of literature in four major ways:

Presents a validated control framework stabilizing microgrid performance under variable operating conditions.

1) Provides a detailed techno-economic analysis based on field data, supporting real-world adoption.
2) Advances dual-mode microgrid modeling, an underexplored area in current renewable energy research.
3) Demonstrates a replicable approach for rural energy planning, particularly in Sub-Saharan Africa, aligning with SDG 7 for clean and affordable energy access.

The remainder of this paper is organized as follows: Section II outlines the methodology used for system modeling, simulation, and techno-economic analysis. Section III discusses the results, including validation, comparison with existing literature, and implications for rural electrification.

The paper concludes in Section IV by summarizing key findings and proposing future research directions.

II. THEORETICAL AND CONCEPTUAL FRAMEWORK

A. Optimization Problem Formulation

The design and operation of the microgrid renewable energy system are formulated as a constrained optimization problem aimed at achieving three key objectives: minimizing the Levelized Cost of Energy (LCOE), ensuring system reliability, and maximizing renewable energy utilization. This formulation explicitly defines the decision variables, constraints, and operational logic that govern microgrid performance, providing a clear and systematic framework for both technical and economic optimization.

1) Objective Function:

$$Minimize: LCOE = \frac{NPC}{\sum_t^T L\ (t)\Delta t} \quad (1)$$

Subject to the following constraints:

a- Load Following Constraint: Diesel generation operates only when renewable generation and battery storage cannot meet the load demand:

$$P_{\text{GEN}}(t) \geq L(t) - \Big(P_{\text{PV}}(t) + P_{\text{WT}}(t) + P_{\text{BATT,discharge}}(t)\Big), \forall t \quad (2)$$

b- Battery Priority Constraint: Excess renewable energy charges the battery before supplying the load:

$$P_{\text{BATT,charge}}(t) = \max\big(0, P_{\text{PV}}(t) + P_{\text{WT}}(t) - L(t)\big), \forall t \quad (3)$$

c- Renewable Fraction Constraint: At least 70% of annual energy must come from solar PV and wind:

$$\frac{\sum_{t=1}^{T}(P_{\text{PV}}(t) + P_{\text{WT}}(t)) \cdot \Delta t}{\sum_{t=1}^{T} L(t) \cdot \Delta t} \geq 0.7 \quad (4)$$

d- Loss of Load Probability (LOLP) Constraint: The probability of unmet load must remain below 1%:

$$LOLP = \frac{\sum_{t=1}^{T} E_{\text{deficit}}\ (t)}{\sum_{t=1}^{T} L(t) \cdot \Delta t} \leq 0.01 \quad (5)$$

e- Battery Depth of Discharge (DoD) Constraint: Battery usage is limited to prolong lifespan:

$$SOC_{\text{min}} \geq (1 - DoD_{\text{max}}) \cdot SOC_{\text{rated}}, DoD_{\text{max}} = 0.8 \quad (6)$$

f- Component Capacity Constraint: System components must operate within rated capacities.

$$0 \leq P_{\text{PV}}(t) \leq P_{\text{PV,max}}, 0 \leq P_{\text{WT}}(t) \leq P_{\text{WT,max}}, 0 \leq P_{\text{BATT}}(t) \leq P_{\text{BATT,max}}, 0 \leq P_{\text{GEN}}(t) \leq P_{\text{GEN,max}} \quad (7)$$

Where:

- NPC: Net present cost
- L (t): Case study load demand at time (t)
- Δt: Time interval
- $P_{\text{GEN}}(t)$: Power output of the diesel generator at time step t(kW). Determines the backup energy supplied when renewables and batteries cannot meet load demand.
- $L(t)$: Load demand at time step t(kW). Represents the electricity requirement of the case study community over the simulation period.
- $P_{\text{PV}}(t)$: Power output of the photovoltaic system at time step t(kW). Indicates the solar energy contribution to the load.
- $P_{\text{WT}}(t)$: Power output of the wind turbine at time step t(kW). Represents the wind energy supplied to the system.
- $P_{\text{BATT,discharge}}(t)$: Battery discharge power at time t(kW). Energy supplied by the battery to the load during periods of low renewable generation.
- $P_{\text{BATT,charge}}(t)$: Battery charging power at time t(kW). Energy stored in the battery from excess renewable generation.
- SOC_{min}: Minimum state of charge of the battery (kWh). Ensures the battery does not discharge beyond allowable depth.
- SOC_{rated}: Rated (maximum) battery capacity (kWh). Used to calculate allowable Depth of Discharge (DoD).
- DoD_{max}: Maximum allowable depth of discharge (%). Limits battery cycling to prolong lifespan.
- $E_{\text{deficit}}(t)$: Energy deficit at time step t(kWh). Represents unmet load when generation and storage cannot satisfy demand.
- $LOLP$: Loss of Load Probability (%). The probability of the system failing to meet load demand, used to ensure reliability.
- $P_{\text{PV,max}}, P_{\text{WT,max}}, P_{\text{BATT,max}}, P_{\text{GEN,max}}$: Maximum rated capacities (kW)

This formulation provides a transparent and systematic optimization framework, linking technical constraints, operational priorities, and economic objectives. It explicitly demonstrates how system components are coordinated (PV, WT, BESS, diesel generator, inverter) to achieve a reliable, cost-effective, and high-renewable microgrid design.

B. Modeling the MG Distributed Energy Resources (DERs)

In engineering, modeling involves representing physical systems using mathematical expressions that define the characteristics of individual components and the relationships that govern their interactions (Maślak & Orłowski, 2022; Kreishan & Zobaa, 2023). A microgrid system comprising DERs, storage devices, and loads is mathematically modeled for both islanded and grid-connected operations, accurately representing component characteristics and interconnections to determine output power (Rao & Kumar, 2021).

1) Modeling the Photovoltaic (PV) Power Plant

Photovoltaic solar panels are key renewable energy sources due to their unlimited supply, environmental benefits,

and ability to generate electricity, heat, and light (Abedrabboh et al., 2022; Rice et al., 2023). PV cells, typically made from amorphous or monocrystalline silicon, efficiently convert sunlight into electricity over extended periods. Factors such as insolation, temperature, and cell efficiency affect power conversion (Regany et al., 2025). Common applications include satellite systems, water pumping, lighting, and battery charging.

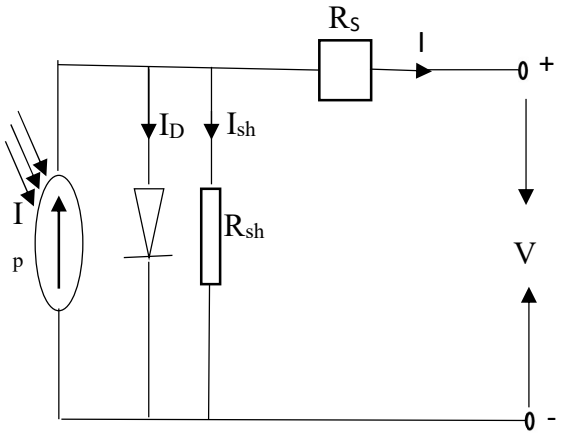

Figure 1 Equivalent circuit model of a PV cell

A one-diode model can be used to describe the equivalent circuit diagram of a PV solar cell, as shown in Figure 1 (Obiwulu et al., 2022). The PV cell is represented as a combination of a diode and a current source, with Rs denoting the series resistance. The total current is calculated using equations (8) and (9) (Venkateswari & Rajasekar, 2021).

$$I = I_{ph} - I_D \quad (8)$$

$$I = I_{ph} - I_O\left(e^{\frac{e(V+IR_S)}{mkT_C}} - 1\right) \quad (9)$$

Parameters for PV Cell Modeling:
m: Ideality factor, represents the efficiency of the PV cell's diode behavior,
K: Boltzmann constant: Describing the relationship between temperature and energy at a microscopic level ($1.38 * 10^{-2}\ j/k$).
T_C : The PV cell's absolute temperature in Kelvin,
e : Charge of an electron ($1.602 * 10^{-19}C$)
V: The applied voltage across the PV cell,
I_o: Reverse saturation current when the cell is in darkness

A module is created when PV cells are connected. The module's short-circuit current and open-circuit voltage are influenced by the configuration of its cells, specifically the number of cells connected in parallel and in series (Bui et al., 2024). In addition to sunlight, other environmental factors that significantly affect voltage and current levels include ambient temperature and irradiance. The current of a PV module can be calculated using the following formula:

$$I_m = N_C^P I_C^{SC}\left[1 - \exp\left(\frac{V_m - N_C^S V_C^{OC} + \frac{I_m R_C^S}{N_C^P}}{N_C^S V_C^t}\right)\right] \quad (10)$$

Where:
I_m: Current of the module, V_m = Voltage of the module, N_C^P: The total number of cells in parallel, N_C^S = The total number of cells in series, I_C^{SC}: The cells short-circuit current, V_C^{OC}: The cell's open-circuit voltage, V_C^t: Thermal voltage of the cell, define as $V_C^t = \frac{mKT_C}{e}$.
Alternatively, the induced voltage across the module can be estimated as:

2) Boosting the PV output power using the Perturb and Observe method

The power output of solar cells varies with temperature and solar insolation, impacting their current- voltage properties. This work utilizes the Perturb and Observe (P&O) method (Remoaldo & Jesus, 2021; Aicha et al., 2025) to optimize the maximum power output of PV systems.

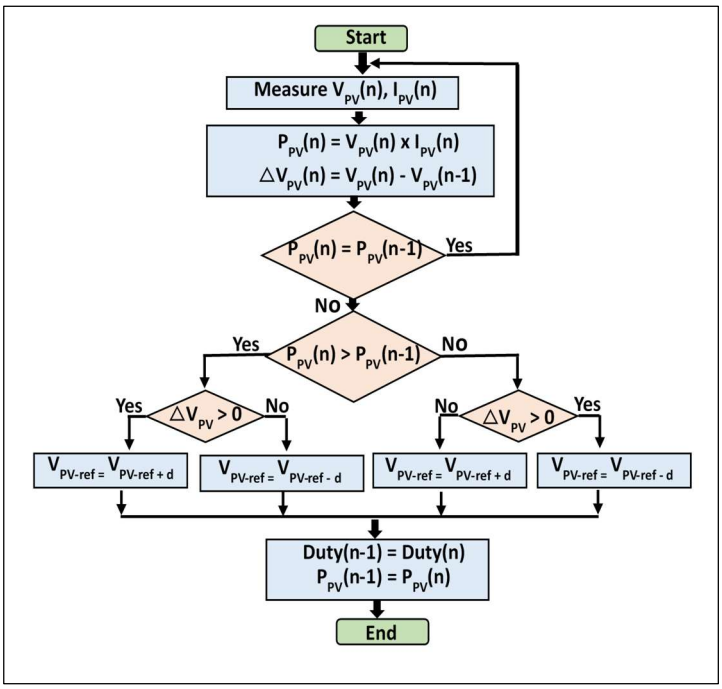

Figure 2 Flowchart of the P&O

Incrementally adjusting the PV voltage and observing the resulting change in power to track the maximum power point (MPP). It begins by measuring the photovoltaic voltage $V_{PV}(n)$ and current $I_{PV}(n)$, then calculates the power $P_{PV}(n)$. The PV power $P_{PV}(n)$ is compared with the previous power $P_{PV}(n-1)$.

If power increases with a positive voltage change ($\Delta VPV>0$), the algorithm continues increasing the voltage (i.e., perturbs in the same direction). If power decreases, the direction of the perturbation is reversed. The reference voltage V_{PV}_ref is updated accordingly, and previous values are stored for the next iteration. This process is repeated iteratively to

keep the operating point near the MPP by "perturbing" and "observing" the effect on power.

3) Three-phase inverter modeling

The inverter is an electrical device that converts DC power into AC power with the required voltage and frequency (Mokhtari et al., 2024). In a microgrid, the inverter connects the DC renewable energy source to the AC systems that link the loads to the utility grid. It plays a vital role in controlling and stabilizing voltage, frequency, active power, and reactive power within the microgrid systems (Fani et al., 2022). A thorough understanding of inverter management is essential for ensuring the stable operation of micro-generators and, consequently, the entire microgrid. The circuit model of a typical three-phase voltage source inverter is illustrated in Figure 3.

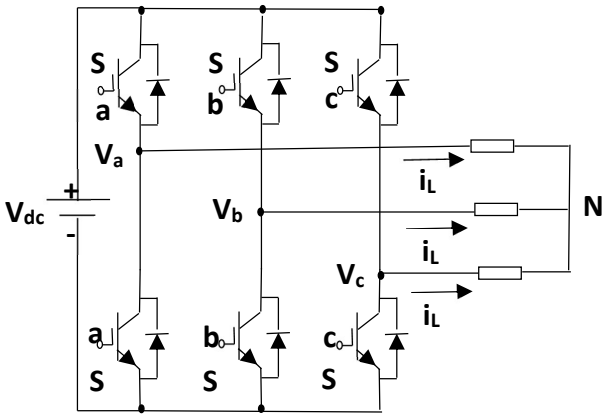

Figure 3 Three-phase voltage-source inverter

The circuit architecture shown in Figure 3 is a straightforward arrangement of three single-phase inverters connected in parallel. It functions similarly to a single-phase inverter, but each arm's gating signals are delayed by 120° with the others to produce a three-phase balanced voltage(Gupta & Singh, 2021). This can be achieved by controlling the six transistors and six diodes in the inverter circuit, ensuring that the two switches in a single arm are never turned on or off simultaneously. The space vector for this type of inverter is given by equation 11.

$$V = \frac{2}{3}\left(V_a + aV_b + a^2 v_c\right) \quad (11)$$

Where:

$$a = exp\left(\frac{j2\pi}{3}\right) \quad (12)$$

This space vector representation applies to both star-connected and delta-connected loads. For a star load, the total phase voltages at the load, whether in balanced or unbalanced conditions, sum to zero:

$$V_a + V_b + V_c = 0 \quad (13)$$

The phase voltage at the load can be expressed as presented in equation 14.

$$V_i = V_j - V_{nN} \quad (14)$$

Where:

i: a, b, c, j: A, B, C, n: the load's neutral point, N: The inverter's negative rail for the DC bus.

The voltages at A, B, and C can now be used to express VnN using equations (15) and (16) as follows:

$$V_a + V_b + V_c = 0 = V_A - V_{nN} + V_B - V_{nN} + V_C - V_{nN} \quad (15)$$

$$V_{nN} = \frac{1}{3}(V_a + V_b + V_c) \quad (16)$$

Therefore, the phase-to-neutral voltage at the load can be represented using equations (17).

$$\begin{aligned} V_a &= \frac{2}{3}V_A + \left(-\frac{1}{3V_B} - \frac{1}{3V_C}\right) \\ V_b &= \frac{2}{3}V_B + \left(-\frac{1}{3V_C} - \frac{1}{3V_A}\right) \\ V_c &= \frac{2}{3}V_C + \left(-\frac{1}{3V_B} - \frac{1}{3V_A}\right) \end{aligned} \quad (17)$$

4) Modeling the Wind Energy Conversion System

Kinetic energy is converted into electrical energy by a wind turbine. Several variables, including air density, wind direction, site altitude, surrounding topography, and temperature, influence the amount of electricity that wind systems can generate in specific locations (Alotibe & Crebbin, 2010). The power output curve is the most essential technical data for a specific wind turbine, as it illustrates the relationship between wind speed and the generator's electrical output. Figure 4 displays an idealized version of this power curve.

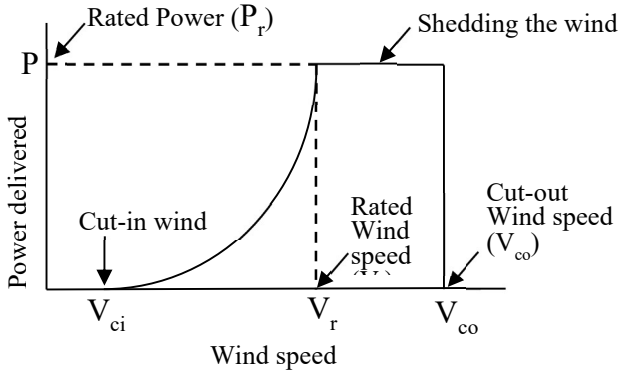

Figure 4 A typical Wind Turbine Power Curve

Typically, the manufacturer's data sheet contains the power output curve for a particular wind turbine. Three important wind speed characteristics affect wind turbine power output: (i) The minimal wind speed needed to produce net power is known as the cut-in wind speed (Vci) since lower wind speeds are insufficient to overcome turbine friction and generate enough electricity. (ii) The wind speed at which the turbine produces its maximum designed power is termed the rated wind speed (Vr) (Umar et al., 2022). To avoid damaging the generator at this speed, techniques like active pitch control and passive stall management are employed. (iii) Cut-out

(Vco), also known as furling wind speed, is the maximum wind speed at which no power is generated, and the turbine must be stopped to prevent damage, and no power is produced above this threshold. The hourly power output of the wind energy system is expressed in equation 18 (Al-Quraan et al., 2022).

$$P^{W} = \begin{bmatrix} 0 & V_W < V_{ci} \text{ or } V_W \geq V_{co} \\ P^{R}\dfrac{V_W - C_{ci}}{V_r - V_{ci}} & V_{ci} \leq V_W \leq V_r \\ P^{R} & V_r \leq V_W \leq V_{co} \end{bmatrix} \quad (18)$$

where:

P^W : The wind energy conversion system's total power output.

P^R : The wind turbine's rated power

V_W : The wind speed at the height of the turbine hub.

V_{ci} : The wind turbine's cut-in wind speed.

V_{co} : The wind turbine's cut-out wind speed.

V_r : The wind turbine's rated wind speed.

The power law equation can be used to determine the wind speed at the wind turbine's hub height (h) and reference height (hr), using the following expression: (19) (XIA et al., 2021).

$$V_W = V_r\left(\frac{h}{h_r}\right)^{\propto} \quad (19)$$

where:

α = The shear coefficient, which ranges from 0.10 – 0.40 (Uwineza et al., 2021; Finnah, 2022).

Equation (20) represents the yearly energy produced by the wind turbine.

$$J^{GW} = P^{W} \times 8760\left(\frac{h}{yr}\right)[kWh] \quad (20)$$

5) Modeling the Battery Energy Storage Systems (BESS)

a- Battery Bank: The following equation, which represents the energy balance relationship between the battery bank and the overall energy demand of the microgrid (MG) system, can be used to estimate the battery bank's level of charge (Adesina et al., 2025).

i. The battery bank's state of charge: When other distributed energy sources, such as solar, wind, hydropower, and biomass, produce more energy than is needed to fulfill the load demand, the battery banks must be charged to store the excess energy. The battery bank's available capacity at hour *h* is as given in equation (21).

$$J^{G_B}(h) = J^{G_B}(h-1) \times (1-\sigma) + \left[J^{G}(h) - \frac{J^{D_M}(h)}{\eta^{inv}}\right] \times \eta^{B} \quad (21)$$

ii- The battery bank's discharge state: In contrast, the battery bank supplies the extra energy needed when the total energy produced by the renewable energy sources is not enough to satisfy the load demand. The battery bank discharges in the process. The battery bank's available capacity at hour *h* can be determined using equation (22):

$$J^{G_B}(h) = J^{G_B}(h-1) \times (1-\sigma) + \left[\frac{J^{D_M}(h)}{\eta^{inv}} - J^{G}(h)\right] \quad (22)$$

where:

$J^{G_B}(h)$: The energy output of the battery bank in kWh per hour.

$J^{G_B}(h-1)$: The energy generation of the battery bank in kWh per hour (h^{-1}).

σ : The self-discharge rate of the battery bank.

$J^{G}(\mathrm{h})$: The self-discharge rate of the battery bank.

$J^{D_M}(h)$: MG system's hourly energy requirement, expressed in kWh.

η^{Inv} : The inverter's efficiency.

η^{B} : The battery bank's charging efficiency

Equation (23) represents the overall amount of energy generated by the renewable MG system in hour *h*, or $J^{G}(\mathrm{h})$.

$$J^{G}(h) = \sum_{i=1}^{NP} J_i^{G_P} + \sum_{i=1}^{NP} J_i^{G_W} \quad (23)$$

where:

$J_i^{G_P}$: The PV module's energy output.

$J_i^{G_W}$:The wind turbine system's energy output.

6) Justification of Algorithm and Technology Selections

This subsection provides the rationale for the selected control algorithms, modulation methods, EMS strategy, and battery technology, ensuring operational reliability, cost-effectiveness, and alignment with the scale and dynamics of the Olowo-Oko microgrid, as supported by recent peer-reviewed studies.

a- MPPT Algorithm: The Perturb and Observe (P&O) method was selected for its simplicity, computational efficiency, and widespread adoption in small- to medium-scale PV systems, particularly for rural microgrids (Ghayth, Yusupov, Hesri, et al., 2023; Al-Quraan & Al-Qaisi, 2021). Compared to Incremental Conductance or fuzzy-logic MPPT methods, P&O offers a robust compromise between tracking accuracy and ease of implementation, making it suitable for the case study.

b- PWM Technique: Triangular Pulse Width Modulation (TPWM) was employed for inverter control, providing reduced harmonic distortion, better power quality, and lower stress on IGBT/diode components (Mohammed & Qasim, 2022; Oleschuk, 2023). While Sinusoidal PWM (SPWM) is also common, TPWM ensures precise modulation index control and simplifies implementation within the microgrid inverter architecture.

c- Energy Management Strategy (EMS): A hierarchical EMS was adopted, prioritizing renewable energy utilization, battery charging from excess generation, and diesel backup only when necessary (Salehi et al., 2022; Abhishek et al., 2020). This approach balances cost-effectiveness, operational reliability, and system resilience. Alternative predictive or AI-based EMS methods require higher computational resources and real-time forecasting, which are less suitable for this community-scale deployment.

d- Battery Technology: Lithium-ion batteries were chosen for their high energy density, long cycle life, and proven performance in hybrid renewable microgrids (Ahmad Khan et al., 2025; Seane et al., 2022; Ngao-det et al., 2025). Although lead-acid batteries are cheaper, their lower lifespan, limited depth of discharge, and higher maintenance make them less appropriate for sustained rural microgrid operation.

III. MATERIALS AND METHODS

A. Data collection

1) Description of the case study site

The Olowo-Oko community serves as the case study for this research. Located in the Asa Local Government Area of Kwara State, Nigeria. The community depends on the conventional national grid for electricity. However, frequent power supply issues underscore the necessity for alternative energy solutions. Positioned at latitude 8°32.2′ N and longitude 4°32.7′ E, the community consists of 125 buildings. Its rich renewable energy resources, such as rivers, biomass, solar, and wind, offer significant potential for sustainable electrification, making it an ideal case study for microgrid modeling and optimization to improve energy access and reliability.

2) Daily energy demand profile of the case study

The case study community's daily load consumption pattern was examined in two distinct scenarios: the rainy season and the dry season. As illustrated in Figure 5, the three-phase Fluke 432-II Power Quality and Energy Analyzer was used to record data on the daily load demand of the community.

Figure 5 Three-phase data logger

In addition to doing load assessments and recording difficult-to-locate voltage occurrences, the data logger can measure power quality. The tool was utilized in this study to calculate the case study's daily energy usage over 24 hours for seven days a week, including the weekend. The SD card fromthe device was used to import recorded data into a laptop for additional examination. The case study community's daily load profile is shown in Figure 6, with average values calculated for each scenario.

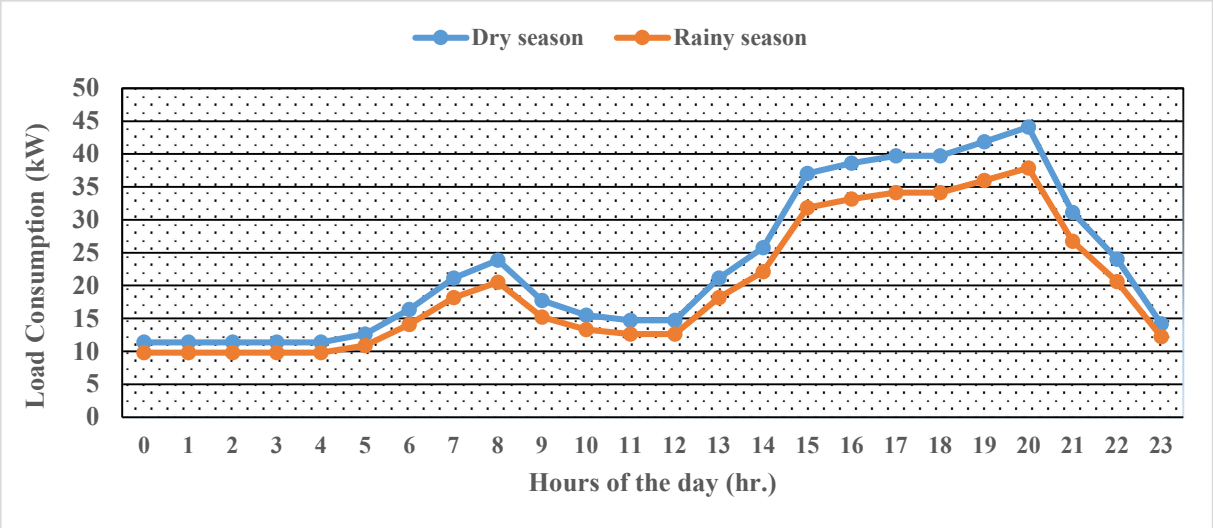

Figure 6 Case study daily load consumption pattern: Dry. Vs Raining season comparison

The Figure shows a consistent yet seasonally varied load pattern, with the dry season recording a higher peak demand of 40.3 kW compared to 36.2 kW in the rainy season, primarily due to increased cooling needs. The daily average load demand is 22.95 kW in the dry season and 19.72 kW in the rainy season. The load analysis reveals a low load factor, with a contrast of approximately 17 kW between average and peak load in both scenarios. This indicates inefficiencies in energy utilization, leading to underutilization of infrastructure during low-demand periods and strain during peak hours. These results highlight the necessity of microgrid interventions to enhance energy management, improve reliability, and integrate renewable energy to meet the community's specific needs effectively.

3) Data sources for wind speed and solar radiance

The case study site's annual profile of solar radiation is shown in Figure 7, while the location's annual average wind speed is presented in Figure 8. These datasets were sourced from the National Aeronautics and Space Administration (NASA) website, which is accessible at

http://eosweb.larc.nasa.gov. The data were generated using the site's latitude and longitude coordinates.

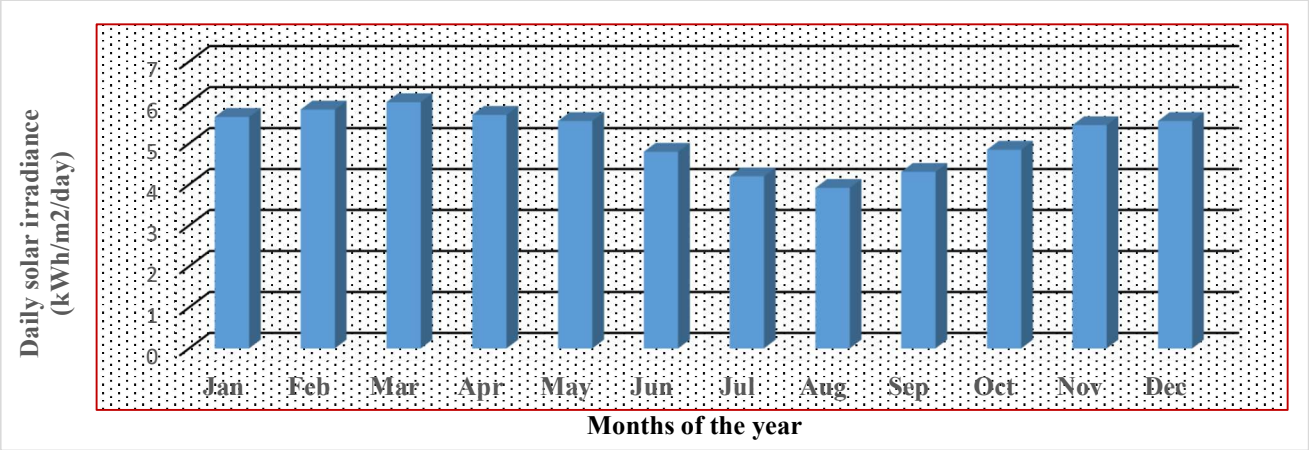

Figure 7 The case study's average solar radiance profile

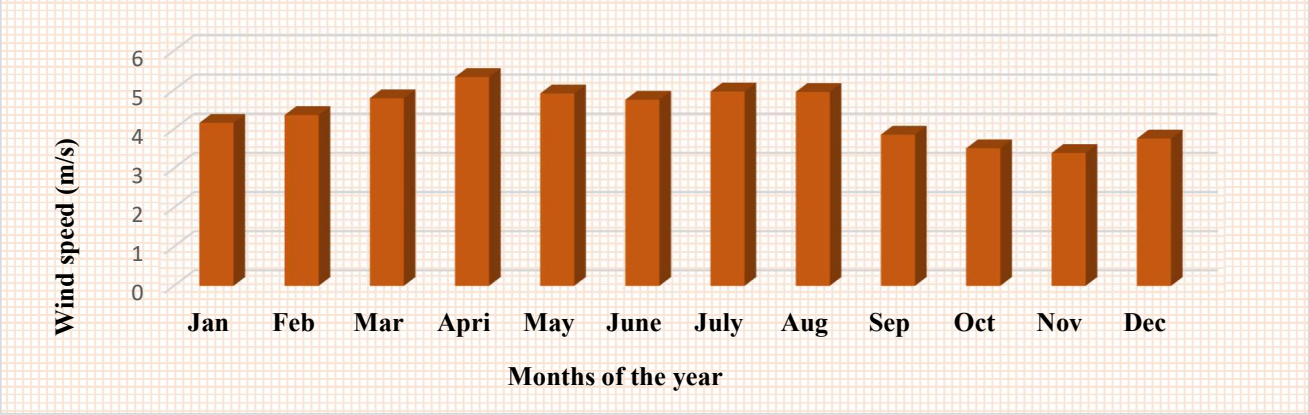

Figure 8 The case study site's average wind speed

Seasonal solar irradiance fluctuation is illustrated in Figure 7, which displays the highest irradiance in March at 6.01 kWh/m²/day and the lowest in August at 3.92 kWh/m²/day. According to these figures, the community gains from increased global solar irradiation and average insulation, supporting the viability of a microgrid power plant. Figure 8 suggests a low wind speed environment, showing a monthly average wind speed of 4.39 m/s at a height of 10 m above ground. While this is not optimal for maximizing wind energy generation, it offers room for future improvement.

B. Overview of the Proposed Microgrid System

The proposed dual-mode renewable microgrid system, depicted in Figure 9, integrates WT, PV systems, and an energy storage unit. These components are connected via converters to a DC bus, which supplies both DC and AC loads through inverters. The energy storage system plays a crucial role in stabilizing voltage and frequency fluctuations while also serving as a backup during insufficient renewable generation.

Energy flow within the MG is bidirectional, allowing surplus power to be stored or redirected. Load controllers manage demand, while real-time communication links enhance system stability. Advanced control strategies, including droop control and virtual inertia, ensure power quality by balancing voltage, frequency, and load variations.

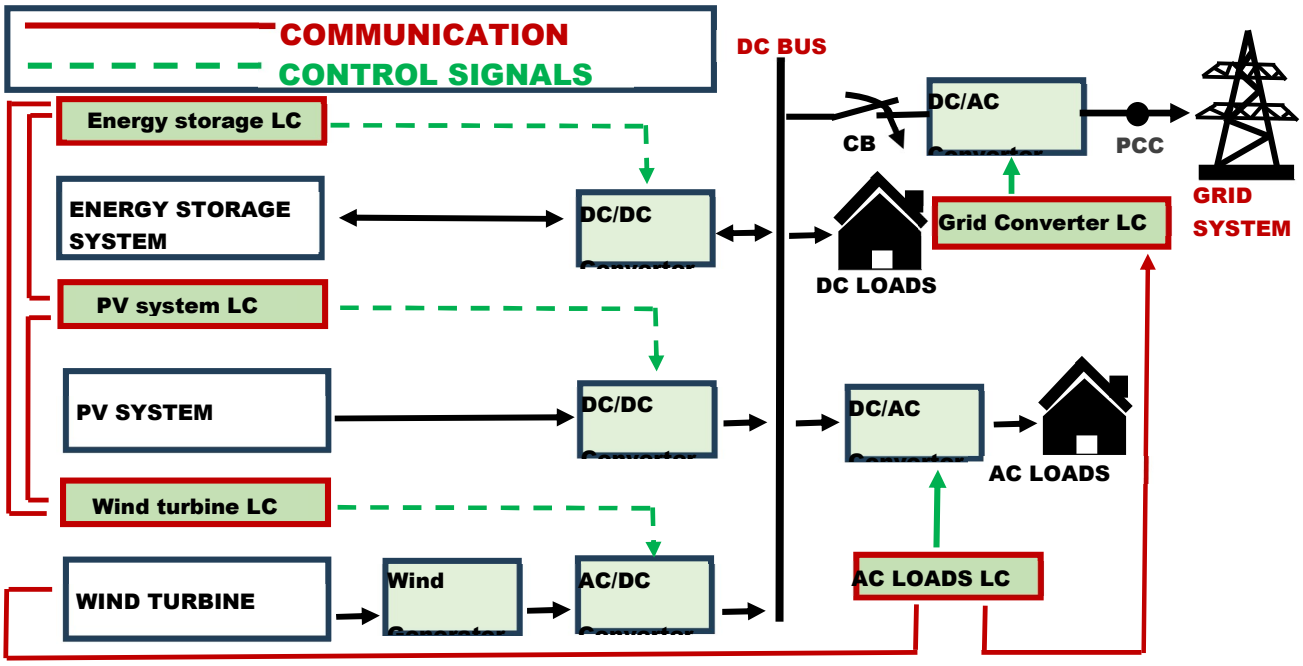

Figure 9 Typical microgrid configuration

The MG connects to the utility grid through a single point of common coupling (PCC), with an isolating circuit breaker (CB) enabling grid separation when necessary. This design enhances stability, reliability, and scalability, addressing key challenges in renewable energy integration and microgrid optimization.

C. Simulation of the proposed Microgrid Systems in MATLAB Simulink

In this work, MATLAB Simulink was utilized as a versatile tool to model and simulate a 40kW/400V microgrid system utilizing renewable energy sources for both stand-alone and grid-connected applications, such as solar wind turbines, PV and BESS. The system integrates components like DC-DC converters, P&O MPP controllers, and inverters, with voltage and frequency control implemented to ensure stability. The case study modeling, as presented in Figure 10**,** incorporates system parameters, daily load profiles, and renewable energy data, with detailed system simulation parameters outlined in Table 1**.** This approach demonstrates the effectiveness of the modeled microgrid for remote and distributed energy applications.

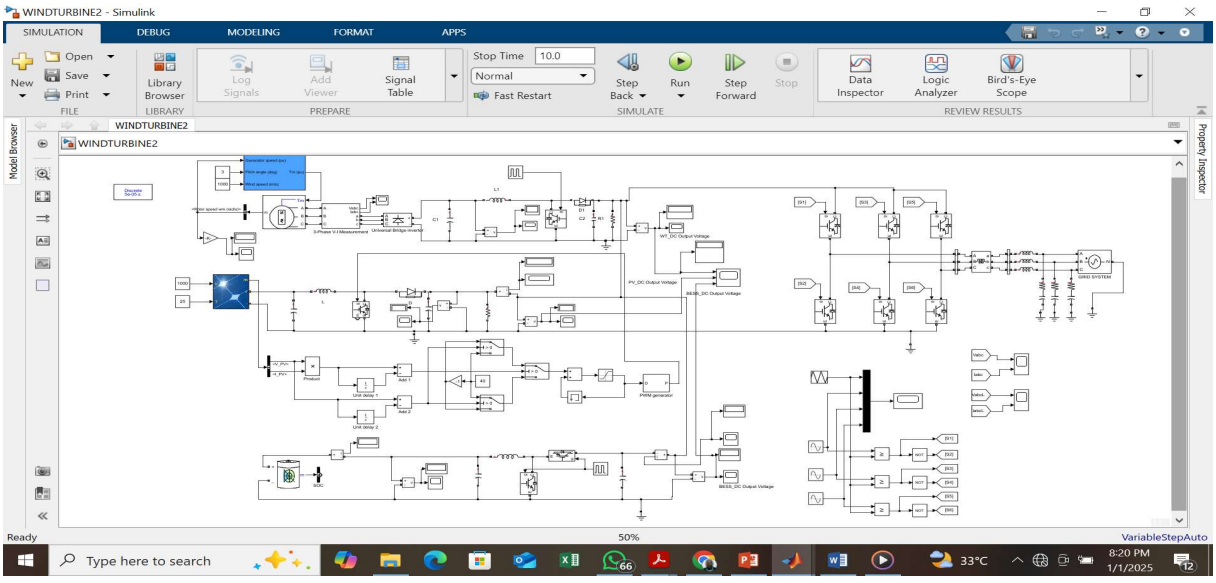

Figure 10 Proposed MG Systems modeling in Malab Simulink

Table 1 MATLAB's Simulation Parameters

Wind Turbine		**DC-DC Boost converter**	
Rated power capacity (kW)	35	Duty cycle (D)	0.4
Rated voltage	400	Inductor (μH)	76.8
Generator Cut-in	2.5	Capacitor (μF)	400
Cut-out speed (m/s)	25	Resistance (Ω)	5
Wind Turbine speed (rpm)	2390	Set. Freq., Fs (kHz)	25
Photovoltaic Cell		**BESS**	
Parallel strings	3	Nominal Vol. (V)	48*687.9
Series module per string	8	Rated capac. (Ah)	48
Max. rated power (kW)	5.1	Initial SOC (%)	100
Voc (V)	36.3	Battery resp. time (s)	30
Ish (A)	7.83	DOD (%)	60
Vmp (V)	232	**System Controller**	
Imp (A)	22.05	Simulation time	10 s – 1 min
Solar Irrad. value	1000 W/m²	Applied MPPT	P&O PWM
PV efficiency (%)/Temp.	95 / 25° C		

D. Energy Management Optimization

This study implements an energy management strategy to optimize power flow among solar PV, wind energy, battery storage, and the load in a dual-mode microgrid. The strategy enhances reliability and operational efficiency by prioritizing renewable generation and regulating energy storage utilization. A battery management system (BMS) monitors the battery's SOC, maintaining it within a safe range of 30% – 90%. A hysteresis-based control algorithm governs charging and discharging, preventing overuse and extending battery life while enabling adaptive load balancing (Gholami et al., 2024; Taye & Choudhury, 2023)**.** The system employs a rule-based optimization technique using real-time inputs such as demand, RES availability, SOC, and grid status to dynamically allocate power, improving energy use, minimizing costs, and enhancing system autonomy (Quizhpe et al., 2024; Hedayatnia et al., 2024)**.** To ensure transparent and reproducible implementation, the EMS is formulated in pseudocode, governing power dispatch among PV, wind, battery, utility grid, and diesel generator based on load demand, renewable availability, operating mode (grid-connected/islanded), and SOC limits:

Initialize SOCmin = 30%, SOCmax = 90%

For each simulation time step t = 1 to T:

Measure P_PV(t), P_WT(t), L(t), SOC(t)

If (P_PV(t) + P_WT(t)) ≥ L(t):
Supply load from renewable sources
If SOC(t) < SOCmax:
Charge battery using excess renewable power
Else:
Curtail excess power or export to grid (grid-connected mode)
Else:
If SOC(t) > SOCmin:
Discharge battery to meet load deficit
Else:
Dispatch diesel generator to supply remaining demand

If grid-connected mode:
Allow power import/export based on system power balance

End For

Maximum Power Point Tracking (MPPT) using the Perturb and Observe (P&O) method enhances solar energy harvesting via DC-DC converters, improving energy extraction and system stability (Prabhakar et al., 2025). This coordinated framework of predictive logic, BMS control, and MPPT integration contributes significantly to operational robustness and economic viability, particularly for remote and off-grid microgrids (Sarang et al., 2024).

E. HOMER Pro Simulation

The PV/WT/BESS system configuration developed in MATLAB Simulink for the case study was cross-verified using HOMER software under two operational modes: Off-Grid and Grid-connected. This verification aimed to assess system performance and feasibility in line with the study's objectives. HOMER allows detailed simulation and sensitivity analysis of hybrid renewable energy systems when provided with appropriate input data.

1) Mode 1: Off-Grid Modeling Scenario

The system's component capacities, capital costs, renewable energy resource data, and daily load profiles for the case study were entered into HOMER's simulation interface, as presented in Figure 11. The simulation was conducted using the

boundary conditions and parameters summarized in Table 2. These parameters define the technical, economic, and operational constraints within which the system optimization was carried out, ensuring accurate and realistic modeling of system behavior over the 25-year project lifetime.

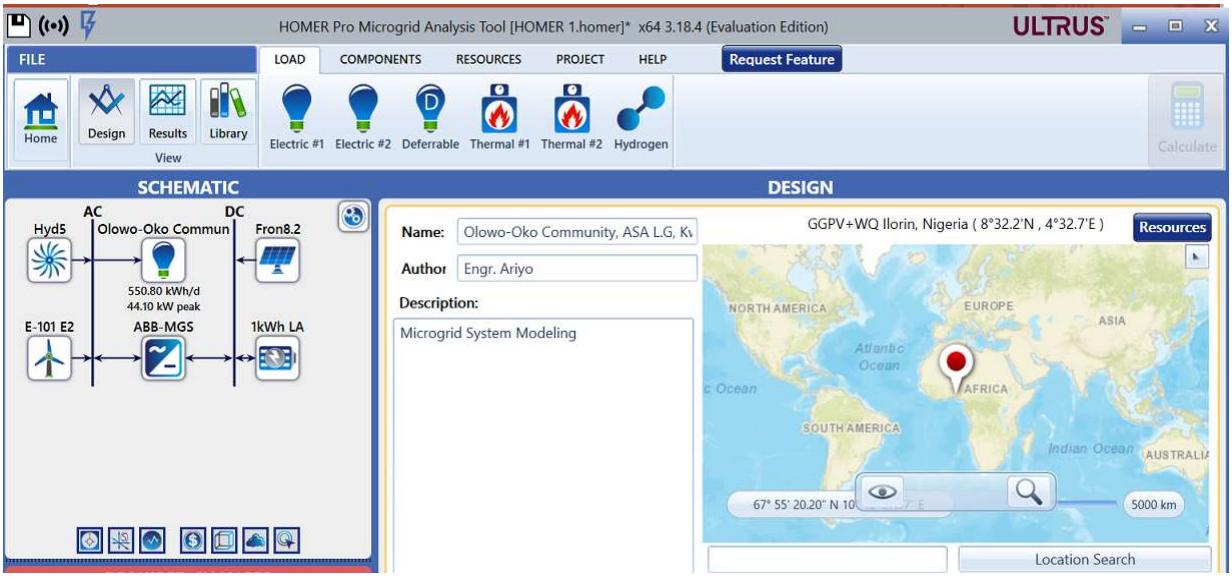

Figure 11 Proposed hybrid system configuration for simulation

Table 2 HOMER Pro's Simulation parameters

Simulation time step	**30 minutes**
Project life time	25 years
Annual interest rate	27.50%
Maximum renewable fraction	98%
Maximum Annual capacity shortage	2%
Dollar Exchange rate	₦1,630 / $

The HOMER simulations use a 27.5% annual interest rate and a specific exchange rate to reflect Nigeria's high lending rates and currency fluctuations (Olurinola & Egbe, 2024; Nwakarame & Awogbemi, 2024). This ensures realistic techno-economic evaluation for metrics such as LCOE, payback period, and net revenue. The project lifetime is explicitly set to 25 years, aligning with typical microgrid horizons and supporting long-term economic calculations including LCOE, NPC, and cumulative revenue.

2) Mode 2: Grid integration Scenario

In the second operational mode, a grid-connected configuration was modeled in HOMER Pro to assess the technical and economic performance of the grid integrated renewable MG systems. The simulation was configured to permit bidirectional power flow, enabling both import from and export to the utility grid. Input parameters included the system load profile, available generation resources, and their respective technical and economic characteristics. Grid interaction settings were defined to facilitate evaluation of operational dynamics within the integrated microgrid framework. Four key performance indicators were used for this assessment: total energy production (kWh/year), percentage of renewable energy fraction, energy purchased from the grid, and energy sold to the grid. For clarity, these indicators were analyzed in pairs. Figure 12 illustrate the HOMER Pro grid-mode simulation platform.

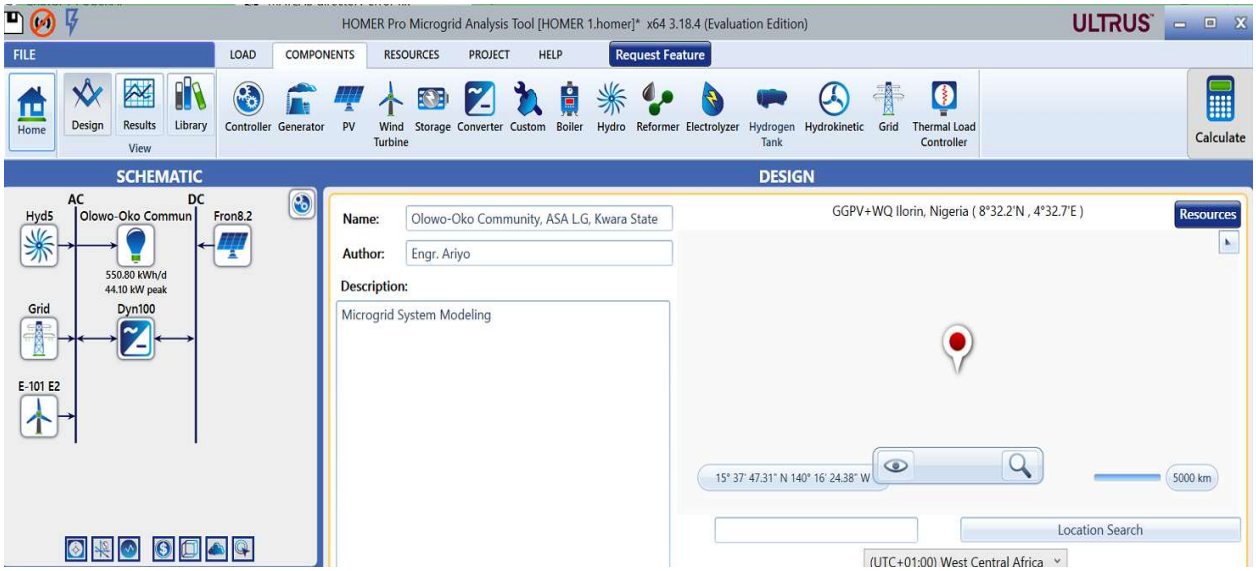

Figure 12 HOMER Pro GRID-MODE Simulation platform

F. Payback Period Estimation for the Optimal System Configuration

The payback period measures how quickly an investment recovers its capital cost through annual savings or revenues, such as energy sales, feed-in tariffs, or incentives. In microgrid optimization, it's a vital financial metric assessing investment attractiveness, risk, and economic resilience. A shorter payback enhances project appeal, supports financial planning, improves bankability, and informs policy and investment decisions.

Payback period is defined as presented in equation (24) (Anselma et al., 2023)

$$\text{Payback Period} = \frac{\text{Capital Cost}}{\text{Annual revenue or saving}} \quad (24)$$

$$\text{Revenue per year} = \text{LCOE} \times \text{Annual Energy Production} \quad (25)$$

Hence.

From the HOMER Pro optimal system configuration cost details, we have:

Total Capital Cost: \$540,994.35,

LCOE: \$0.033/kWh,

Annual energy production: 2,042,373 kW/yr,

Therefore.

$$\text{Revenue per year} = 0.033 \times 2{,}042{,}373 = 67{,}398.309\ \$/\text{yr} \quad (26)$$

Substituting this data in equation (27) gives:

$$\text{Payback Period} = \frac{540{,}994.35}{67{,}398.309} = 8.02 \approx 8 \text{ years } 10 \text{ days} \quad (27)$$

The Payback Period is approximately 8years 10 days.

IV. RESULT AND DISCUSSION

A. MATLAB Simulation Results

Figure 13 presents the dynamic DC output voltage profiles of the WT, PV, and BESS systems over a minute simulation period in the MATLAB/Simulink environment. The WT voltage starts low and is boosted to stabilize near the desired 400 V DC bus, with minimal ripple indicating effective converter performance.

Figure 13 WT-PV-BESS Output Voltages

The PV output also stabilizes at around 400 V, though with higher initial variability, suggesting a functional but potentially optimizable boost converter. The BESS output exhibits significant initial fluctuations, likely due to internal dynamics or load-sharing transients, but eventually aligns with the 400 V DC bus requirement.

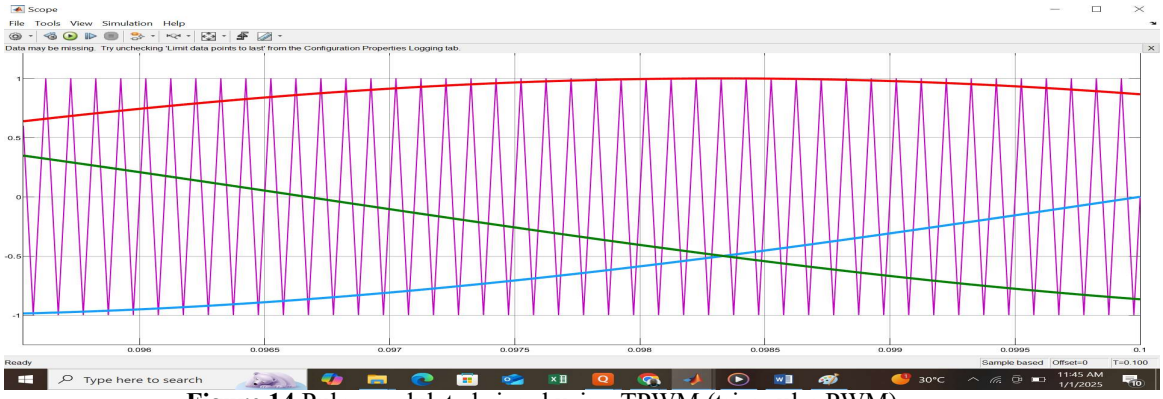

Figure 14 Pulse modulated signal using TPWM (triangular PWM)

TPWM and SPWM are adopted as control signals to the Gate of IGBT/Diode in this work, considering the following benefits it offers:

- ❖ Lower Harmonic Distortion: SPWM minimizes harmonics in the output voltage, leading to smoother and more sinusoidal waveforms.
- ❖ Better Power Quality: Ensures that the voltage supplied to loads closely resembles the ideal AC sinusoidal waveform.
- ❖ Efficient Modulation Index Control: Offers precise control over the modulation index, enabling better amplitude regulation of the output voltage.
- ❖ Reduced Stress on Components: The smoother transitions in SPWM switching signals result in less stress on power electronics like IGBTs and diodes.

Figure 14 shows the output of a Triangular Pulse Width Modulation system. The TPWM generates pulsating signals to drive the PV to capture MPP, and the inverter in this case. The red and green curves signify positive and negative modulating signals, respectively, while the triangular waveform serves as the carrier signal. The points where the modulating signals intersect with the triangular waveform dictate the timing of the switching events that generate the pulse signal.

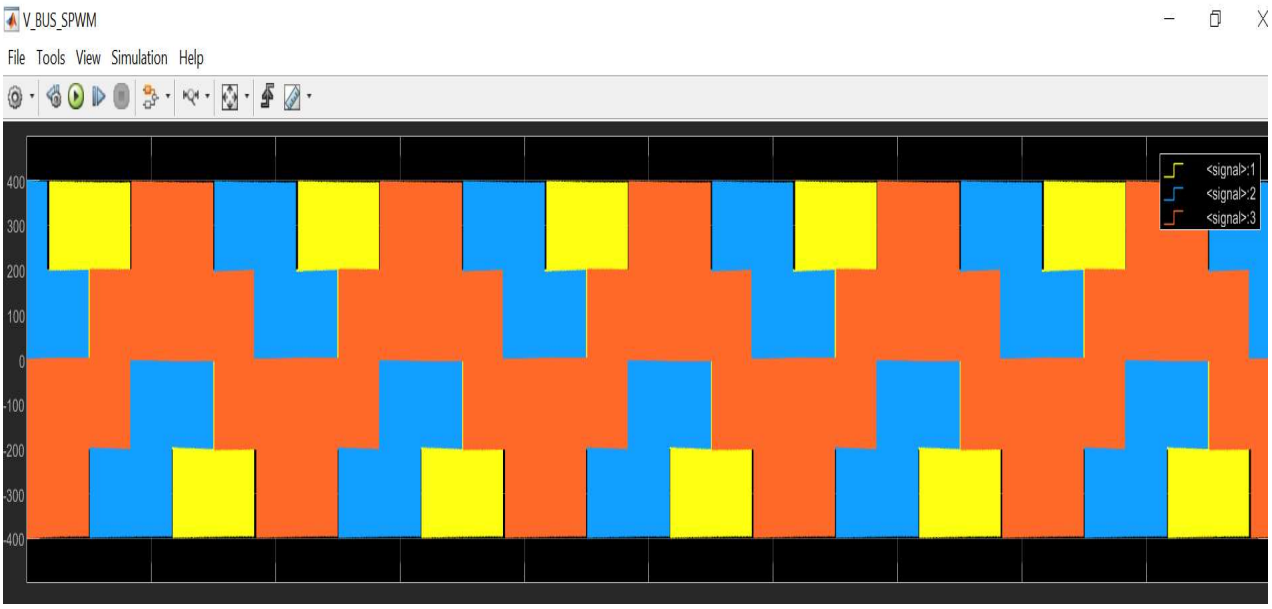

Figure 15 Grid Bus voltage with pulsation and harmonics

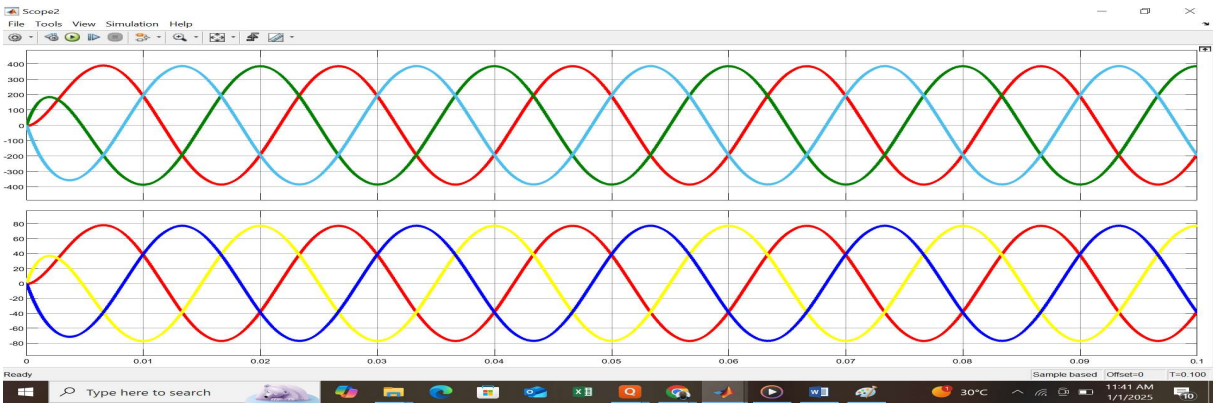

Figure 15 Grid Bus Voltage After applying passive filter

Figures 15 and 16 respectively present the grid system bus voltage before and after the application of a passive filter to mitigate system harmonics. The rectangular, multi-level waveforms in Figure 15 correspond to the output of a voltage source inverter or a power converter. The multiple colors (orange, blue, yellow) represent the three-phase signals being synthesized. Pulsations and distortions in the signal waveform result in harmonics, which degrade voltage quality, impact sensitive loads, cause losses in transmission lines and negatively affect the overall operation of the microgrid (MG) if not mitigated.

The sinusoidal waveforms in Figure 16 depict the grid output voltages after filtering and smoothing with a passive filter at the inverter output to suppress higher-order harmonics. The application of an LC filter ensures proper synchronization of the inverter output with the grid, minimizing phase mismatches and transient distortions.

B. HOMER Results

HOMER Pro was used to simulate various configuration scenarios of renewable energy resources. Three major performance indices-Levelized Cost of Energy (LCOE), Net Present Cost (NPC), and System Capital Cost (SCC)-were employed to evaluate and identify the most cost-effective and reliable hybrid configuration that meets the load demand of the case study. The results of these performance metrics are illustrated in Figures 17, 18, and 19, respectively.

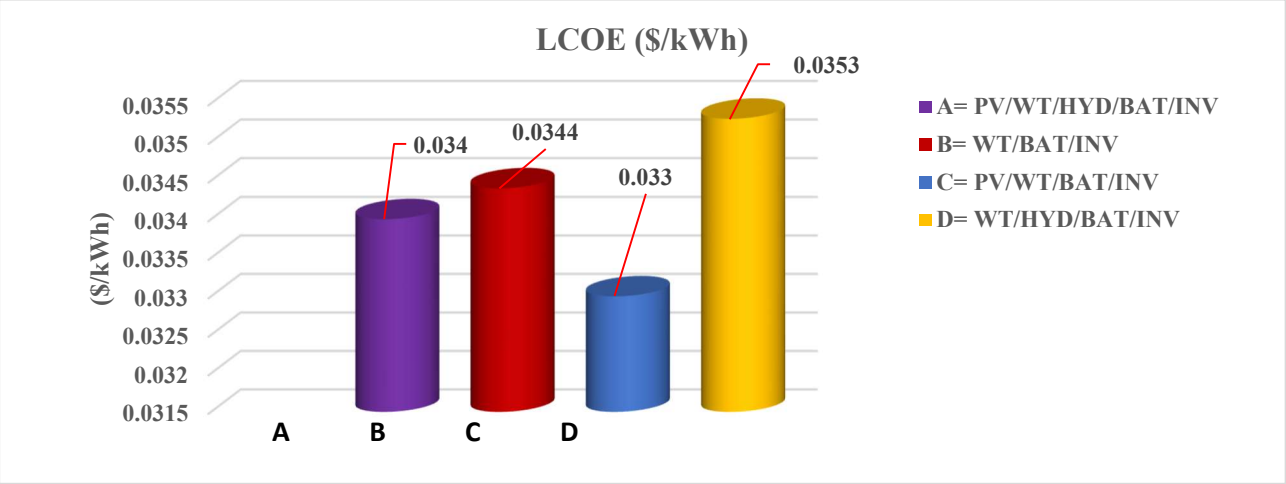

Figure 17 System Configuration Versus Levelized LCOE

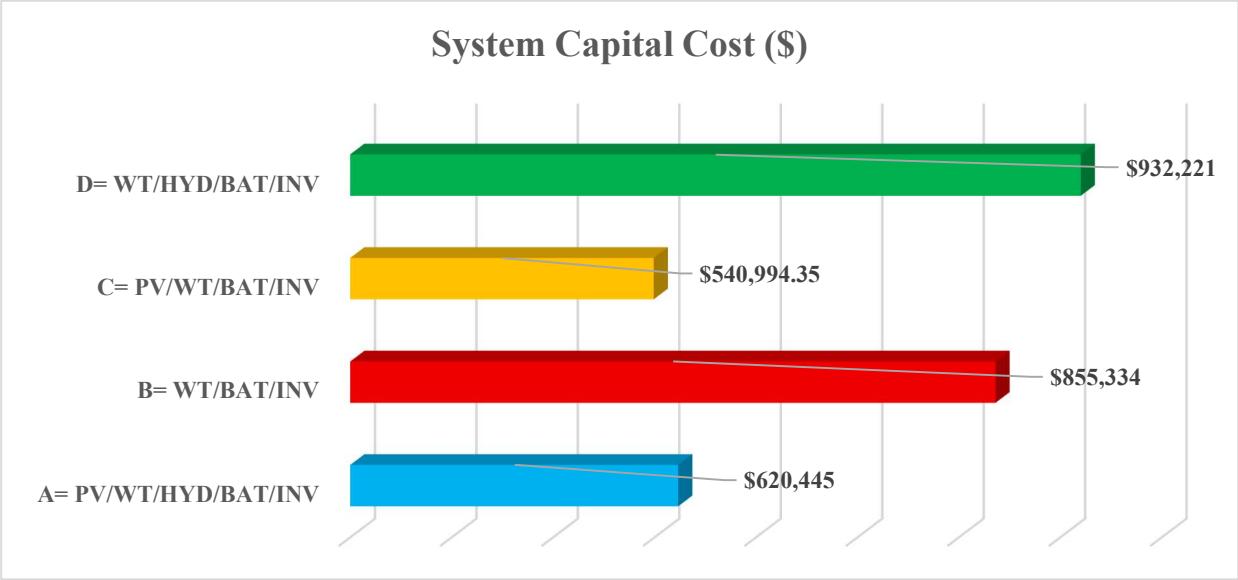

Figure 18 System configurations versus Capital Cost

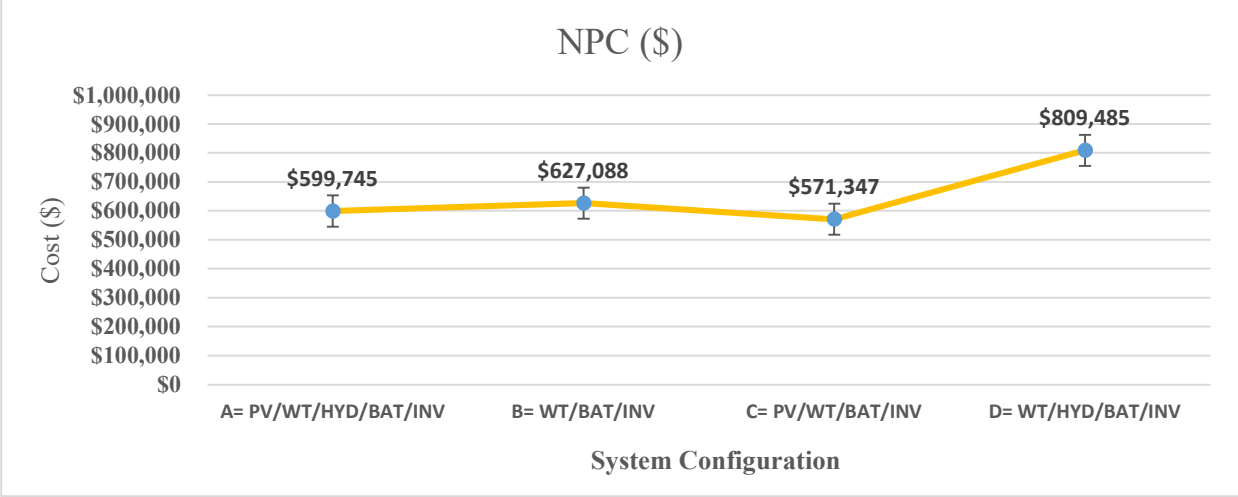

Figure 19 System configurations versus net present cost

From Figure 17, it can be established that system configuration "C" has the lowest LCOE (0.033 $/kWh) among all presented options. This suggests that, in terms of energy cost over the system's lifetime, the combination of PV/WT/BAT/INV is the most economically efficient choice for the case study. For the various system configuration options taken into consideration throughout the simulation, the total capital cost is shown in Figure 18. The lowest capital cost is $540,994.35 for PV/WT/BAT/INV. It is well known that when compared to systems with greater capital costs, those with lower capital costs generate more profit. System capital cost is a significant index for system optimality, particularly in the initial investment phase of a project. A lower capital cost means less upfront financial outlay, which can make a project more attractive and feasible, especially for investors or organizations with budget constraints. It directly impacts the initial financial burden and can influence the project's overall return on investment (ROI). The optimality of the PV/WT/BAT/INV configuration is consolidated by Figure 19, as it presents the lowest NPC of $571,347. It minimizes the total lifetime financial burden of the microgrid system compared to other configurations and also provides a holistic economic assessment, enhancing project feasibility and attractiveness.

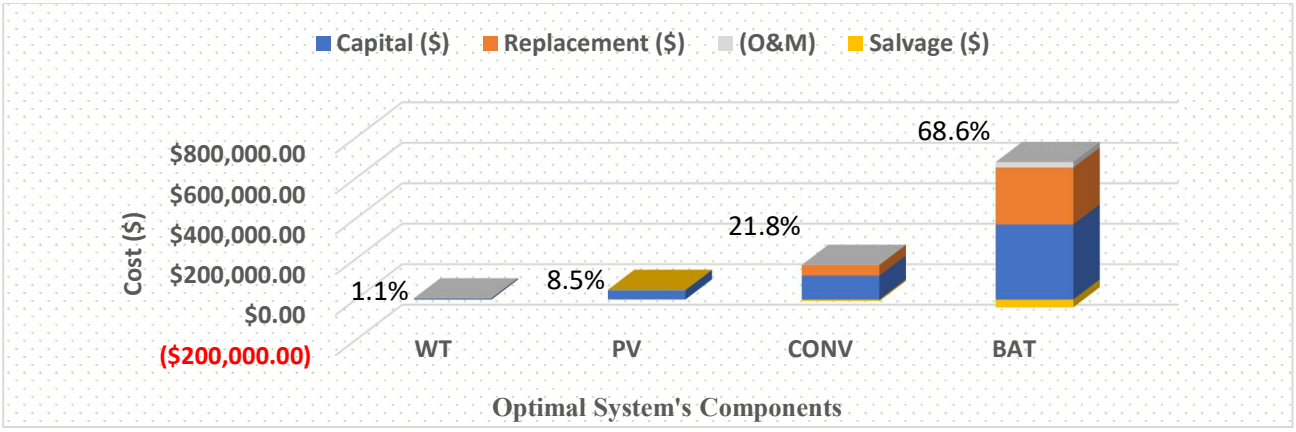

Figure 20 Optimal System Capital Cost Summary

Having established the PV/WT/BAT/INV configuration as the optimal among the four scenarios considered, it is necessary to further determine which component of Scenario "C" is the costliest. Consequently, Figure 20 presents the optimal system capital cost analysis. It can be established from the Figure that the optimal system is battery-heavy dominated with almost 69% of the capital investment, converter coming as the second largest at an approximate worth of 22%, while PV and WT stand at 8.5% and 1.1% respectively. The dominance of battery and inverter costs in the system capital expenditure arises both from their relatively high market prices-exacerbated by currency fluctuations and technology costs-and from the system's operational needs for energy storage and complex AC/DC conversion to manage renewable intermittency and ensure power quality.

C. Sensitivity Analysis Results

To assess the economic resilience of the optimal microgrid configuration, a sensitivity analysis was performed on key parameters affecting the LCOE. This analysis evaluates the influence of battery cost reductions, PV capacity expansion, battery lifespan extension, and changes in discount rate, offering critical insights for investment optimization, risk mitigation, and long-term project sustainability. Multiple sensitivity scenarios were explored to understand how key variables affect LCOE.

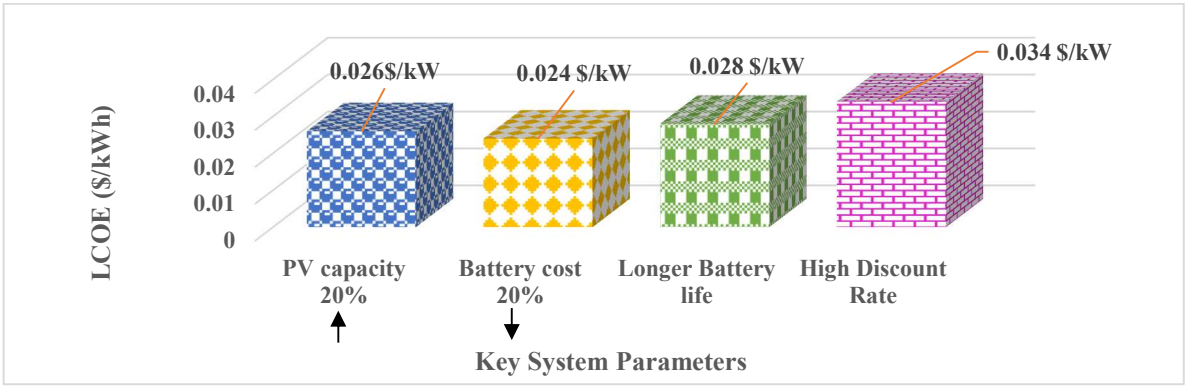

Figure 21 Impact of Sensitivity Analysis on LCOE

The sensitivity analysis presented in Figure 21 highlights how key system parameters influence the LCOE, directly impacting the economic viability of the proposed microgrid. A 20 % reduction in battery cost lowers the LCOE to $0.024/kWh, while a 20 % increase in PV capacity further reduces it to $0.026/kWh, demonstrating the strong cost-saving potential of advancing technologies. Extending battery lifespan also enhances system economics, though moderately, reducing LCOE to $0.028/kWh. Conversely, an increase in the discount rate slightly raises the LCOE, underscoring the importance of favorable financing conditions for microgrid sustainability. These insights not only affirm the robustness of the optimized system but also guide future policy, investment, and technology priorities, thereby reinforcing the relevance and originality of this research. Overall, the analysis indicates that battery cost and lifetime are the most influential parameters, and future advancements in energy storage technologies will be crucial in further reducing microgrid LCOE.

D. Homer Pro Grid-Mode Result

Figure 22 presents the annual energy production and renewable fraction analysis for grid-connected configurations of the optimal system under various scenarios, as modeled in HOMER Pro's Grid mode.The findings offer insights into how hybrid MG systems can be optimally configured to leverage both renewable resources and grid availability for sustainable energy delivery.

As shown in Figure 22, this optimal system configuration yields approximately 3,084,832 kWh/year of energy production with a renewable fraction of 96.8%, underscoring the effective synergy between solar and wind generation when supported by inverters and grid backup.

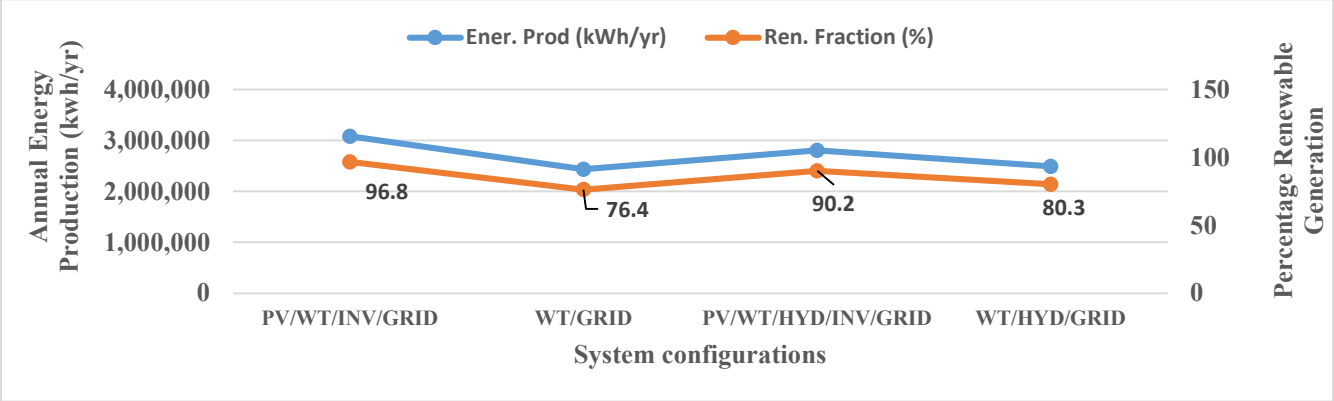

Figure 22 Annual Energy Production and Renewable Fraction Analysis for Grid-Connected System Configurations

In contrast, WT/GRID and WT/HYD/GRID systems produce lower outputs-2.43 and 2.49 million kWh/year, respectively-with reduced renewable fractions of 76.4% and 80.3%, limited by wind variability and hydro seasonality. The PV/WT/HYD/INV/GRID system provides a balanced yet slightly less productive outcome. These findings validate the optimization strategy, emphasizing that systems combining PV, wind, storage, and advanced control technologies maximize both energy output and grid resilience, offering scalable, sustainable solutions for rural electrification and broader renewable energy integration.

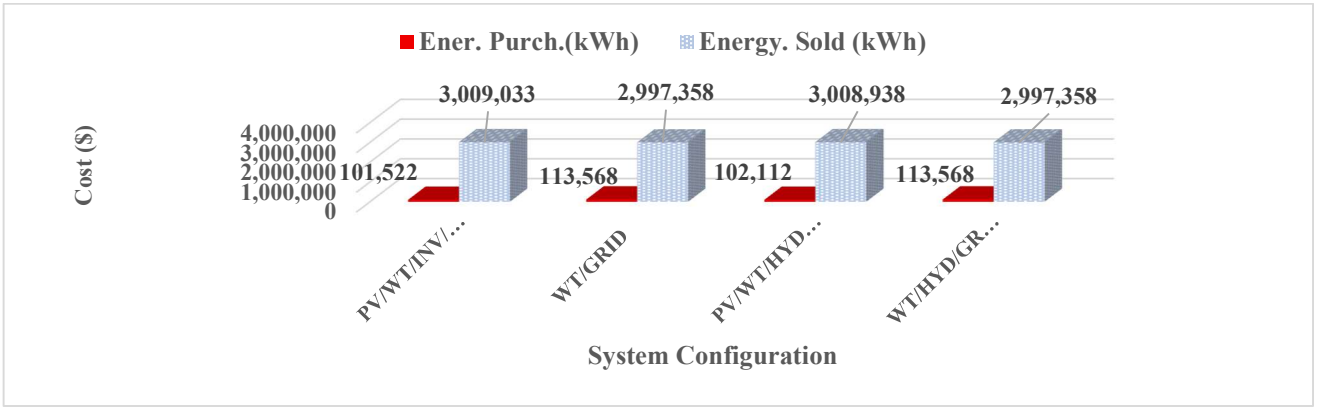

Figure 23 Energy Purchase Versus Sale in Grid-Connected Scenarios

E. Energy Purchase and Sale in Grid-Mode Scenario

The simulation results presented in **Figure 23** offer a comparative evaluation of energy transactions (purchases and sales) across different hybrid system configurations under the grid-integrated application. The PV/WT/INV/GRID configuration records the highest energy export (3,009,033 kWh) and the lowest grid purchase (101,522 kWh), indicating superior renewable generation capacity and minimal dependence on the grid. Both WT/GRID and WT/HYD/GRID configurations exhibit identical performance, selling 2,997,358 kWh and purchasing 113,568 kWh, suggesting that the addition of hydro contributes marginal value when paired with wind alone. The PV/WT/HYD/INV/GRID configuration demonstrates moderate performance, exporting 3,008,938 kWh and importing 102,112 kWh-slightly below the PV/WT/INV/GRID system. These results demonstrate the strategic importance of photovoltaic input, inverter integration, and optimal resource synergy in enhancing microgrid energy trade performance.

F. Time-Series Performance Assessment Result

This section presents the time-series performance assessment of the optimized microgrid configuration using HOMER Pro, evaluating hourly energy generation, storage behavior, grid transactions, and overall system balance to validate operational feasibility and economic robustness.

Figure 24 Optimal System time series output performance

Figure 24 presents a one-month time-series analysis (June 27–July 26, 2024) of a Microgrid's PV-WT-BAT-INV dynamic behavior, simulated in HOMER Pro, reflecting rainy-season conditions. The upper subplot shows PV generation (Green line) peaking above 200 kW midday, dropping on cloudy days. The Total Electrical Load Served (Dark blue Line) remains stable, between 35-50 kW. The Tesla battery Powerwall (Black line) efficiently manages this, charging during solar overproduction and discharging when generation is low, ensuring load leveling with minimal unmet demand. The lower subplot details wind turbine output (Purple Line), occasionally peaking around 900 kW during wind surges, strongly correlating with wind speed variations. This complements solar generation, enhancing reliability, especially at night or on cloudy days. The battery further boosts system stability, supporting self-consumption and reducing grid reliance. These operational insights are crucial for developing advanced control strategies in MATLAB Simulink. This time-series data also serves as a vital benchmark for validating Simulink-based modeling, confirming energy balance, control responsiveness, and technical feasibility, thus reinforcing the research's originality and robustness.

G. Result Validation: Simulink Versus Homer Pro

To establish confidence in the accuracy of the developed microgrid model, a robust cross-validation was conducted using both HOMER Pro and MATLAB Simulink platforms.

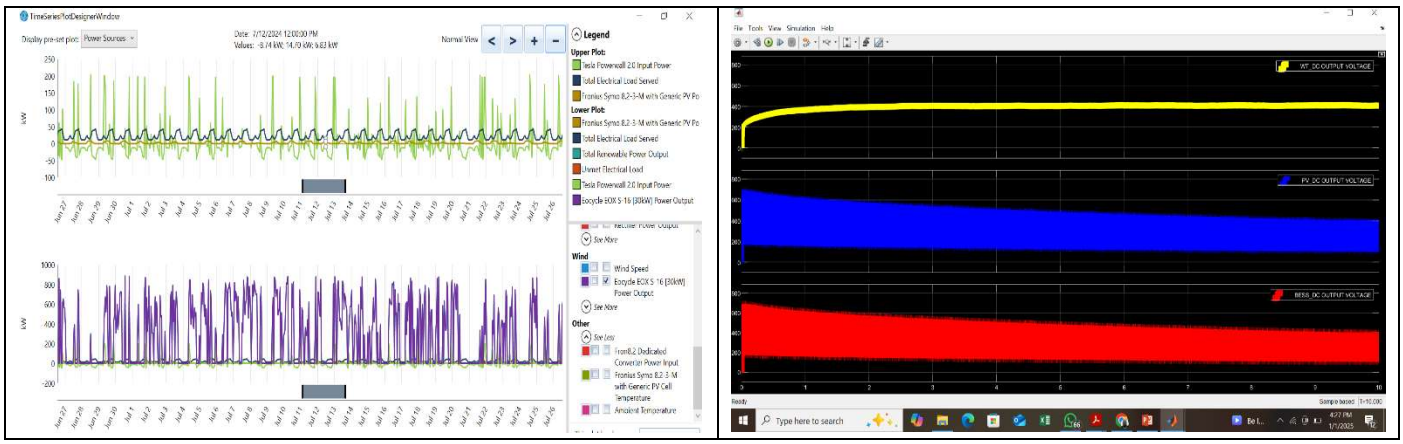

Figure 26 Validity Assessment: Homer Versus MATLAB Simulink

HOMER Pro, as a long-term techno-economic optimization tool, provided resource scheduling, load-following, and energy balancing across a representative operational window. Simultaneously, the Simulink model was developed to capture real-time dynamic behavior including voltage stabilization, frequency regulation, and inertia response under identical load and resource conditions. As shown in Figure 25, the HOMER Pro time series output demonstrates that the microgrid effectively meets demand using variable renewable sources (PV and Wind), supported by battery storage, and inverter system. The corresponding Simulink dynamic simulation validates that the designed control architecture maintains system stability, with WT, PV, BESS, and converters regulating their DC output voltages close to 400V under changing inputs.

Table 3 Validation Appraisal outcome

Validation Parameter	HOMER Pro (Time Series)	Simulink Output (Dynamic Stability)	Observation/Validation
Optimality System configuration	PV/WT/BAT/INV	PV/WT/BAT/INV	Both simulation tools confirm PV/WT/BAT/INV as optimal system config.
PV Power Output	Clear daily cycle trend, Daily max ~200 kW.	Boost converter regulates PV voltage to ~400V DC bus after initial fluctuations.	Both simulation software tools confirm PV output voltage stability.
Wind Power Output	Intermittent, fluctuating between 0–900 kW, reflecting variable wind resource.	Boost converter stabilizes wind input to 400V DC bus with minimal ripple.	Wind turbine fluctuation performance is established in both MATLAB Simulink and Homer Pro.
Battery Storage Dynamics	Charge/discharge cycles responding to excess generation and load demand; SOC dynamically managed.	BAT voltage initially unstable but stabilizes to 400V DC bus after transient adjustments.	Both tools show dynamic SOC regulation and voltage stabilization post-transients.
Total Load Demand	Fairly constant daily load approximately (80–120 kW); no unmet load recorded.	System load shared across sources; Simulink ensures dynamic balancing of power under all load conditions.	Both models match load consumption demand.
System Stability (Voltage & Frequency)	HOMER assumes stable system voltage/frequency but does not simulate real-time dynamics.	Simulink confirms voltage regulation at 400V and frequency stability at 50 Hz across varying conditions.	Simulink strengthens HOMER's feasibility claim by proving actual voltage and frequency stability during operation.

The validation appraisal in Table 3 confirms consistency between both models across key performance indices. HOMER Pro shows long-term energy balance, while the Simulink model validates real-time dynamic stability, maintaining a stable 400V DC bus and 50 Hz frequency under fluctuating PV, wind, and load. This integrated approach affirms the proposed microgrid's operational feasibility and addresses the research gap in hybrid renewable microgrid stability and control.

H. Comparative Analysis of Results with Relevant Literature

Table 4 presents a comparative analysis of the key findings from this study against relevant existing literature. It highlights areas of alignment, improvements, and novel contributions, particularly in MPPT techniques, control strategies, operational flexibility, and economic viability of microgrid systems. (Rashwan et al., 2023; Wang et al., 2024)

.

Table 4 Comparative Analysis of Results with Relevant Literature

Focus Area	Findings from this Study	Relevant Literature	Comparison & Contribution
MPPT Technique (P&O)	Demonstrated effective use of the P&O method in maximizing PV output under varying conditions.	Mohammed et al. (2022)	This study corroborates existing results by showing the practical application of the P&O algorithm with improved solar output.
Operational Mode	Introduced a dual-mode microgrid system (grid-connected and islanded) ensuring voltage and frequency stability during dynamic switching.	Safder et al. (2024)	Offers a more robust and flexible approach to microgrid operation, overcoming the single-mode limitations in prior models.
Wind Integration	Achieved stable wind turbine integration with minimal voltage ripple and consistent performance.	Gholami et al. (2022)	Demonstrates enhanced wind energy performance and improved voltage quality, in contrast to prior findings of fluctuating efficiencies.
Control Strategy & Inverter Design	Implemented advanced modulation and inverter-based control (e.g., TPWM, SPWM) to handle renewable intermittency and ensure dynamic stability.	Sahoo et al. (2025)	Advances beyond traditional droop control by integrating modulation-based and hybrid simulation-hardware approaches for frequency and inertia management.
Grid Synchronization	Explored TPWM and SPWM for optimal synchronization, ensuring smooth transition and efficient operation.	Rashwan et al. (2023)	Provides novel insight into PWM strategies to improve grid interfacing and synchronization in renewable-based MGs.
Cost-Benefit Implications for Rural Settings	Demonstrated high renewable fraction, low LCOE, and feasible payback period, reinforcing technical and economic viability for rural electrification.	Wang et al. (2024)	Validate earlier-economic feasibility studues, while offering greater cost efficiency and practical recommendations for rural microgrid deployment.

I. Comparison with Real-Life Scenarios

The outcomes of this research align closely with real-life rural electrification challenges and are supported by similar field-based studies in sub-Saharan Africa. For instance, (Yimen et al., 2018) analyzed a hybrid off-grid system comprising PV, wind, biogas, and pumped-hydro storage for a rural community in northern Cameroon. Their study demonstrated that such a system could reliably meet rural energy demands while minimizing Net Present Cost and ensuring sustainability-findings that strongly corroborate the techno-economic and operational performance of the microgrid model developed in this research. Both studies emphasize the importance of optimizing renewable resource integration and storage to provide stable, cost-effective, and clean energy access in remote communities, thereby affirming the real-world applicability of the proposed system.

J. Limitations and Future Work

1) Limitations This study successfully developed and validated a dual mode microgrid system, but its scalability and

broader applicability face several limitations. The model was geographically specific to the Olowo-Oko community's dynamics (40 kW/400 V), requiring significant recalibration for different regions or larger scales. The control framework was simplified, using P&O and droop control, lacking more advanced adaptive or AI-based strategies for enhanced responsiveness. Hardware-in-the-Loop (HIL) validation was not conducted due to resource constraints, limiting insights into practical challenges beyond simulation. Furthermore, the study did not include a comprehensive assessment of community acceptance and social sustainability or a deeper analysis of broader environmental impact and policy dimensions. Lastly, the model lacked real-time communication technologies and cybersecurity considerations. These limitations highlight key areas for future research, focusing on scaling, intelligence, and interdisciplinary analysis.

2) Future work

While this study focused on the Olowo-Oko community as a rural case, the developed microgrid architecture is adaptable to diverse geographic and climatic contexts. Future research will explore scalability across multi-village clusters, performance under low irradiance, high humidity, and variable wind. Advancements will include hybrid and AI-based control strategies for real-time forecasting and power-sharing optimization. The integration of IoT-enabled battery management systems (BMS) is also envisioned to improve system responsiveness. Economic viability studies will assess capital costs, long-term savings, and deployment feasibility in remote areas. Additionally, environmental and social impact assessments will inform policy and foster community acceptance. These efforts will ensure broader applicability, enhance resilience and support the global shift toward sustainable and decentralized energy solutions in underserved regions.

IV. CONCLUSION AND RECOMMENDATION

A. Conclusion

This study successfully developed and validated an optimized dual-mode microgrid system integrating solar PV, wind turbines, battery storage, and inverter technologies for rural electrification. Using MATLAB Simulink and HOMER Pro, the research demonstrated both the dynamic stability and techno-economic viability of the proposed PV/WT/BAT/INV configuration, achieving a low LCOE of $0.033/kWh, a 8-year 10-days payback period, and over $1.1 million in net revenue over 25 years. By integrating control strategies, real-time modeling, and economic optimization, the research effectively addresses critical gaps in renewable microgrid design, particularly regarding voltage and frequency stability under variable operating conditions. The findings contribute to existing knowledge by presenting a scalable, cost-effective hybrid solution with strong real-world applicability for energy-poor regions.

B. Recommendation

Future research should prioritize hardware-in-the-loop validation to ensure robust real-time system performance. In addition, integrating AI-based control systems can further enhance adaptive stability under dynamic environmental and load conditions. Broader socio-environmental impact assessments are also recommended to guide deployment readiness, strengthen policy integration, and ensure sustainable adoption of hybrid microgrid solutions in similar contexts.

AUTHORS CONTRIBUTIONS

B.O. Ariyo: Conceptualization, Data curation, Formal analysis, Investigation, Methodology, Project administration, Resources, Software, Supervision, Validation, Visualization, Writing-original draft; writing-review and editing.

L.M. Adesina, O. Ogunbiyi, A. Musa, B.J. Ojuolape, M.O. Balogun,: Data curation, Formal analysis, Investigation, Methodology, Project administration, Supervision, Validation, Visualization.

Acknowledgement

The authors sincerely appreciate Engr. Rasheed Olowo, Chairman of the case study community, for his invaluable support during field data collection, which significantly contributed to the success of this research. We also extend our gratitude to the Head of the Department of Electrical and Electronics Engineering, University of Ilorin, for facilitating the release of the Field Data Energy Analyzer used in this study. Furthermore, we express our heartfelt appreciation to the Head of the Data Acquisition Unit, Ilorin NASA Office, whose provision of essential atmospheric data greatly guided this work. To all of you, we deeply acknowledge your support and contributions.

REFERENCES

Abedrabboh, O., Koç, M., & Biçer, Y. (2022). Modelling and analysis of a renewable energy-driven climate-controlled sustainable greenhouse for hot and arid climates. *Energy Conversion and Management*, *273*. https://doi.org/10.1016/j.enconman.2022.116412

Abhishek, A., Ranjan, A., Devassy, S., Kumar Verma, B., Ram, S. K., & Dhakar, A. K. (2020). Review of hierarchical control strategies for DC microgrid. In *IET Renewable Power Generation* (Vol. 14, Issue 10, pp. 1631–1640). John Wiley and Sons Inc. https://doi.org/10.1049/iet-rpg.2019.1136

Adesina, L. M., Ariyo, B. O., Ogunbiyi, O., & Musa, A. (2025). Optimal Analysis of Microgrid (MG) Systems : Modeling and Control Dynamics for Enhanced Performance – A Case Study Approach. *KU8+*, *2*(2), 1–40.

Agha Kassab, F., Rodriguez, R., Celik, B., Locment, F., & Sechilariu, M. (2024). A Comprehensive Review of Sizing and Energy Management Strategies for Optimal Planning of Microgrids with PV and Other Renewable Integration. *Applied Sciences (Switzerland)*, *14*(22), 1–31. https://doi.org/10.3390/app142210479

Ahmad Khan, A., Faiz Minai, A., Godi, R. K., Shankar Sharma, V., Malik, H., & Afthanorhan, A. (2025). Optimal Sizing, Techno-Economic Feasibility and Reliability Analysis of Hybrid Renewable Energy System: A Systematic Review of Energy Storage Systems' Integration. *IEEE Access*, *13*(January), 59198–59226. https://doi.org/10.1109/ACCESS.2025.3535520

Aicha, M. Ben, Hacene, N., & Teta, A. (2025). Comparative study of P & O and PSO-based MPPT algorithms for PV systems under partial shading conditions Comparative study of P & O and PSO-based MPPT algorithms for PV systems under partial shading conditions. *Researchgate*, *June*, 1–9.

Al-Ezzi, A. S., & Ansari, M. N. M. (2022). Photovoltaic Solar Cells: A Review. In *Applied System Innovation* (Vol. 5, Issue 4). MDPI. https://doi.org/10.3390/asi5040067

Al-Mahammedi, M. T. F., & Onat, M. (2025). Optimal Siting, Sizing, and Energy Management of Distributed Renewable Generation and Storage Under Atmospheric Conditions. *Sustainability (Switzerland)*, *17*(1). https://doi.org/10.3390/su17010300

Al-Quraan, A., Al-Masri, H., Al-Mahmodi, M., & Radaideh, A. (2022). Power curve modelling of wind turbines- A comparison study. *IET Renewable Power Generation*, *16*(2), 362–374. https://doi.org/10.1049/rpg2.12329

Al-Quraan, A., & Al-Qaisi, M. (2021). Modelling, design and control of a standalone hybrid PV-wind micro-grid system. *Energies*, *14*(16), 1–23. https://doi.org/10.3390/en14164849

Alam, F., & Jin, Y. (2023). The Utilisation of Small Wind Turbines in Built-Up Areas: Prospects and Challenges. *Wind*, *3*(4), 418–439. https://doi.org/10.3390/wind3040024

Alotibe, M., & Crebbin, G. (2010). *Microgrid: Modelling and Control*.

Andreotti, D., Spiller, M., Scrocca, A., Bovera, F., & Rancilio, G. (2024). Modeling and Analysis of BESS Operations in Electricity Markets: Prediction and Strategies for Day-Ahead and Continuous Intra-Day Markets. *Sustainability*, *16*(18), 7940. https://doi.org/10.3390/su16187940

Anselma, P. G., Kollmeyer, P. J., Feraco, S., Bonfitto, A., Belingardi, G., Emadi, A., Amati, N., & Tonoli, A. (2023). Economic Payback Time of Battery Pack Replacement for Hybrid and Plug-In Hybrid Electric Vehicles. *IEEE Transactions on Transportation Electrification*, *9*(1), 1021–1033. https://doi.org/10.1109/TTE.2022.3202792

Assad, U., Hassan, M. A. S., Farooq, U., Kabir, A., Khan, M. Z., Bukhari, S. S. H., Jaffri, Z. U. A., Oláh, J., & Popp, J. (2022). Smartgrid, Demand Response and Optimization: A Critical Review of Computational Methods. *Energies*, *15*(6), 1–36. https://doi.org/10.3390/en15062003

Bhatti, M. Z. A., Siddique, A., Aslam, W., & Atiq, S. (2024). Design and Analysis of a Hybrid Stand-Alone Microgrid. *Energies*, *17*(1). https://doi.org/10.3390/en17010200

Bilendo, F., Meyer, A., Badihi, H., Lu, N., Cambron, P., & Jiang, B. (2023). Applications and Modeling Techniques of Wind Turbine Power Curve for Wind Farms—A Review. In *Energies* (Vol. 16, Issue 1). MDPI. https://doi.org/10.3390/en16010180

Bui, V. H., Truong, V. A., Nguyen, V. L., & Duong, T. L. (2024). Estimating the potential maximum power point based on the calculation of short-circuit current and open-circuit voltage. *IET Power Electronics*, *17*(3), 402–421. https://doi.org/10.1049/pel2.12651

Djilali, A. B., Yahdou, A., Benbouhenni, H., Alhejji, A., Zellouma, D., & Bounadja, E. (2024). Enhanced perturb and observe control for addressing power loss under rapid load changes using a buck–boost converter. *Energy Reports*, *12*, 1503–1516. https://doi.org/10.1016/j.egyr.2024.07.032

Ebrahimi, A., Attar, S., & Farhang-Moghaddam, B. (2021). A multi-objective decision model for residential building energy optimization based on hybrid renewable energy systems. *International Journal of Green Energy*, *18*(8), 775–792. https://doi.org/10.1080/15435075.2021.1880911

Ekpoh, M. I., Otuagoma, S. O., Ubeku, E. U., & Eyenubo, O. J. (2025). Techno-Economics Analysis of an Off-Grid Hybrid Power System for Rural Areas in Nigeria. *Journal Of Engineering Research Innovation And Scientific Development*, *3*(1), 1–8. https://doi.org/10.61448/jerisd32251

Fani, B., Shahgholian, G., Haes Alhelou, H., & Siano, P. (2022). Inverter-based islanded microgrid: A review on technologies and control. In *e-Prime - Advances in Electrical Engineering, Electronics and Energy* (Vol. 2). Elsevier Ltd. https://doi.org/10.1016/j.prime.2022.100068

Finnah, B. (2022). Optimal bidding functions for renewable energies in sequential electricity markets. *OR Spectrum*, *44*(1), 1–25. https://doi.org/10.1007/s00291-021-00646-9

Ghayth, A., Yusupov, Z., Hesri, A., & Khaleel, M. (2023). Performance Enhancement of PV Array Utilizing Perturb & Observe Algorithm. *International Journal of Electrical Engineering and Sustainability (IJEES)*, *1*(2), 29–37. https://ijees.org/index.php/ijees/index

Ghayth, A., Yusupov, Z., & Khaleel, M. (2023). Performance Enhancement of PV Array Utilizing Perturb & Observe Algorithm. *International Journal of Electrical Engineering and Sustainability (IJEES)*, *1*(2), 29–37.

Gholami, M., Muyeen, S. M., & Lin, S. (2024). Optimizing microgrid efficiency: Coordinating commercial and residential demand patterns with shared battery energy storage. *Journal of Energy Storage*, *88*, 1–14. https://doi.org/10.1016/j.est.2024.111485

Gupta, A., & Singh, O. (2021). Design & Analysis of Grid Tied Single Stage Three Phase PV System. *International Research Journal of Engineering and Technology*. www.irjet.net

He, M., Wang, Y., Song, Z., Tan, Z., Cai, Y., You, X., Xie, G., & Huang, X. (2025). Power Quality Mitigation in Modern Distribution Grids : A Comprehensive Review of Emerging Technologies and Future Pathways. *Processes*, *13*(2615), 1–25.

Hedayatnia, A., Ghafourian, J., Sepehrzad, R., Al-Durrad, A., & Anvari-Moghaddam, A. (2024). Two-Stage Data-Driven optimal energy management and dynamic Real-Time operation in networked microgrid based deep reinforcement learning approach. *International Journal of Electrical Power and Energy Systems*, *160*, 1–19. https://doi.org/10.1016/j.ijepes.2024.110142

Hernández-Mayoral, E., Jiménez-Román, C. R., Enriquez-Santiago, J. A., López-López, A., González-Domínguez, R. A., Ramírez-Torres, J. A., Rodríguez-Romero, J. D., & Jaramillo, O. A. (2024). Power Quality Analysis of a Microgrid-Based on Renewable Energy Sources:

A Simulation-Based Approach. *Computation*, *12*(11), 1–32. https://doi.org/10.3390/computation12110226

Hoarcă, I. C., Bizon, N., Șorlei, I. S., & Thounthong, P. (2023). Sizing Design for a Hybrid Renewable Power System Using HOMER and iHOGA Simulators. *Energies*, *16*(4), 1–25. https://doi.org/10.3390/en16041926

Kareem, P. R., Hasan, F. H., Algburi, S., Ezzat, S. B., & Kareem, P. R. (2025). Investigating the Impact of Internal and External Factors on Solar Cell Performance to Enhance Energy Conversion Efficiency. *IRAQI Academic Scientic Journals*, *8*(1), 14–23.

Kreishan, M. Z., & Zobaa, A. F. (2023). Scenario-Based Uncertainty Modeling for Power Management in Islanded Microgrid Using the Mixed-Integer Distributed Ant Colony Optimization. *Energies*, *16*(10). https://doi.org/10.3390/en16104257

Kumar, P. H., Gopi, R. R., Rajarajan, R., Vaishali, N. B., Vasavi, K., & Kumar P, S. (2024). Prefeasibility techno-economic analysis of hybrid renewable energy system. *E-Prime - Advances in Electrical Engineering, Electronics and Energy*, *7*, 1–19. https://doi.org/10.1016/j.prime.2024.100443

Letzgus, S., & Müller, K. R. (2024). An explainable AI framework for robust and transparent data-driven wind turbine power curve models. *Energy and AI*, *15*. https://doi.org/10.1016/j.egyai.2023.100328

Marti-Puig, P., Hernández, J. Á., Solé-Casals, J., & Serra-Serra, M. (2024). Enhancing Reliability in Wind Turbine Power Curve Estimation. *Applied Sciences (Switzerland)*, *14*(6). https://doi.org/10.3390/app14062479

Maślak, G., & Orłowski, P. (2022). Microgrid Operation Optimization Using Hybrid System Modeling and Switched Model Predictive Control. *Energies*, *15*(3). https://doi.org/10.3390/en15030833

Mazorra-Aguiar, L., Lauret, P., David, M., Oliver, A., & Montero, G. (2021). Comparison of two solar probabilistic forecasting methodologies for microgrids energy efficiency. *Energies*, *14*(6). https://doi.org/10.3390/en14061679

Mohammed, M. F., & Qasim, M. A. (2022). Single Phase T-Type Multilevel Inverters for Renewable Energy Systems, Topology, Modulation, and Control Techniques: A Review. *Energies*, *15*(22), 1–24. https://doi.org/10.3390/en15228720

Mohammed, R. H., Abdulrazzaq, A. A., & Al-Azzawi, W. K. (2022). Benefits of MPP tracking PV system using perturb and observe technique with boost converter. *International Journal of Power Electronics and Drive Systems*, *13*(4), 2468–2477. https://doi.org/10.11591/ijpeds.v13.i4.pp2468-2477

Mokhtari, K., Shokri-Kojori, S., & Aliyari-Shoorehdeli, M. (2024). A new generalized state-space averaged model, control design and stability analysis for three phase grid-connected quasi-Z-Source inverters. *International Journal of Electrical Power and Energy Systems*, *158*. https://doi.org/10.1016/j.ijepes.2024.109932

Nadzim, M., Yusoof, M., Iqbal Zakaria, M., Farina Shair, E., Khalid, N. S., Rahman, A., & Emhemed, A. A. (2023). Investigating the Effectiveness of Maximum Power Point Tracking (MPPT) with Perturb and Observe (P&O) Algorithm in Solar Power Battery Charging System. In *Journal of Engineering Research and Education* (Vol. 15).

Ngao-det, M., Thongpron, J., Namin, A., Patcharaprakiti, N., Muangjai, W., & Somsak, T. (2025). Systematic Optimize and Cost-Effective Design of a 100% Renewable Microgrid Hybrid System for Sustainable Rural Electrification in Khlong Ruea, Thailand. *Energies*, *18*(7), 1–35. https://doi.org/10.3390/en18071628

Nur-e-alam, M., Abedin, T., Samsudin, N. A., & Petrů, J. (2025). Optimization of energy management in Malaysian microgrids using fuzzy logic-based EMS scheduling controller. *Scientific Reports*, *15*(995), 1–15.

Nur-E-Alam, M., Abedin, T., Samsudin, N. A., Petrů, J., Barnawi, A. B., Soudagar, M. E. M., Khan, T. M. Y., Bashir, M. N., Islam, M. A., Yap, B. K., & Kiong, T. S. (2025). Optimization of energy management in Malaysian microgrids using fuzzy logic-based EMS scheduling controller. *Scientific Reports*, *15*(1), 1–15. https://doi.org/10.1038/s41598-024-82360-4

Nwakarame, I. P., & Awogbemi, T. O. (2024). *Exchange Rate Volatility on Economic GrowtThe Impact of Foreign h of Nigeria*. *10*(4), 215–227.

Obiwulu, A. U., Erusiafe, N., Olopade, M. A., & Nwokolo, S. C. (2022). Modeling and estimation of the optimal tilt angle, maximum incident solar radiation, and global radiation index of the photovoltaic system. *Heliyon*, *8*(6). https://doi.org/10.1016/j.heliyon.2022.e09598

Odoi-Yorke, F., & Woenagnon, A. (2021). Techno-economic assessment of solar PV/fuel cell hybrid power system for telecom base stations in Ghana. *Cogent Engineering*, *8*(1), 1–25. https://doi.org/10.1080/23311916.2021.1911285

Oleschuk, v. (2023). Evolution and dissemination of specialized strategies, methods, and techniques of synchronous pulsewudth modulation for control of voltage source inverters and inverter-based systems. *Technical Electrodynamics*, *2023*(5), 14–27. https://doi.org/10.15407/techned2023.05.014

Olurinola, I. O., & Egbe, I. E. (2024). *Examining the Effects of Fiscal-Monetary Policy Interactions on Unemployment Rates in Nigeria (1985-2023)*. *8*(9), 1–16. https://doi.org/10.47772/IJRISS

Prabhakar, D., Nagaraja, S., Koundinya, S. P., & Meghana, R. (2025). Power Extraction in Photovoltaic Systems using P&O-Based MPPT with DC-DC Buck Converter Integration. *WSEAS Transactions on Electronics*, *16*, 46–50. https://doi.org/10.37394/232017.2025.16.6

Quizhpe, K., Arévalo, P., Ochoa-Correa, D., & Villa-Ávila, E. (2024). Optimizing Microgrid Planning for Renewable Integration in Power Systems: A Comprehensive Review. *Electronics*, *13*(18), 1–30. https://doi.org/10.3390/electronics13183620

Rao, K. S., & Kumar, Y. V. P. (2021). Comprehensive Modelling of Renewable Energy Based Microgrid for System Level Control Studies. *International Journal of Renewable Energy Research*, *11*(1), 223–234. https://doi.org/10.20508/ijrer.v11i1.11745.g8127

Rashwan, A., Mikhaylov, A., Senjyu, T., Eslami, M., Hemeida, A. M., & Osheba, D. S. M. (2023). Modified

Droop Control for Microgrid Power-Sharing Stability Improvement. *Sustainability (Switzerland)*, *15*(14), 1–19. https://doi.org/10.3390/su151411220

Regany, D., Palau, F. M., Crespo, A., Barrau, J., Vilarrubí, M., & Rosell-Urrutia, J. (2025). Enhancing efficiency of dense array CPV receivers with controlled DC-DC converters and adaptive microfluidic cooling under non-uniform solar irradiance. *Solar Energy Materials and Solar Cells*, *279*. https://doi.org/10.1016/j.solmat.2024.113262

Remoaldo, D., & Jesus, I. S. (2021). Analysis of a traditional and a fuzzy logic enhanced perturb and observe algorithm for the mppt of a photovoltaic system. *Algorithms*, *14*(1), 1–19. https://doi.org/10.3390/a14010024

Rice, I. K., Zhu, H., Zhang, C., & Tapa, A. R. (2023). A Hybrid Photovoltaic/Diesel System for Off-Grid Applications in Lubumbashi, DR Congo: A HOMER Pro Modeling and Optimization Study. *Sustainability (Switzerland)*, *15*(10). https://doi.org/10.3390/su15108162

Salehi, N., Martinez-Garcia, H., Velasco-Quesada, G., & Guerrero, J. M. (2022). A Comprehensive Review of Control Strategies and Optimization Methods for Individual and Community Microgrids. *IEEE Access*, *10*, 15935–15955. https://doi.org/10.1109/ACCESS.2022.3142810

Sarang, S. A., Raza, M. A., Panhwar, M., Khan, M., Abbas, G., Touti, E., Altamimi, A., & Wijaya, A. A. (2024). Maximizing solar power generation through conventional and digital MPPT techniques : a comparative analysis. *Scientific Reports*, *14*(8944), 1–18. https://doi.org/10.1038/s41598-024-59776-z

Sawadogo, B., Benmouna, A., Becherif, M., Barakat, S., & Samy, M. (2025). Integrated solar electrification and community empowerment in a burkina faso Village: A feasibility and design study. *Results in Engineering*, *27*, 1–18. https://doi.org/10.1016/j.rineng.2025.105686

Seane, T. B., Samikannu, R., & Bader, T. (2022). A review of modeling and simulation tools for microgrids based on solar photovoltaics. In *Frontiers in Energy Research* (Vol. 10). Frontiers Media S.A. https://doi.org/10.3389/fenrg.2022.772561

Singh, K. M., & Gope, S. (2021). Renewable energy integrated multi-microgrid load frequency control using grey wolf optimization algorithm. *Materials Today: Proceedings*, *46*, 2572–2579. https://doi.org/10.1016/j.matpr.2021.02.035

Taye, B. A., & Choudhury, N. B. D. (2023). Adaptive filter based method for hybrid energy storage system management in DC microgrid. *E-Prime - Advances in Electrical Engineering, Electronics and Energy*, *5*, 1–13. https://doi.org/10.1016/j.prime.2023.100259

Twaisan, K., & Bar, N. (2022). Integrated Distributed Energy Resources (DER) and Microgrids: Modeling and Optimization of DERs. In *Electronics (Switzerland)* (Vol. 11, Issue 18, pp. 1–24). MDPI. https://doi.org/10.3390/electronics11182816

Umar, D. A., Yaw, C. T., Koh, S. P., Tiong, S. K., Alkahtani, A. A., & Yusaf, T. (2022). Design and Optimization of a Small-Scale Horizontal Axis Wind Turbine Blade for Energy Harvesting at Low Wind Profile Areas. *Energies*, *15*(9). https://doi.org/10.3390/en15093033

Uwineza, L., Kim, H. G., & Kim, C. K. (2021). Feasibilty study of integrating the renewable energy system in Popova Island using the Monte Carlo model and HOMER. *Energy Strategy Reviews*, *33*, 100607. https://doi.org/10.1016/j.esr.2020.100607

Vaish, J., Tiwari, A. K., & Siddiqui, K. M. (2023). Optimization of micro grid with distributed energy resources using physics based meta heuristic techniques. *IET Renewable Power Generation*, 1–17. https://doi.org/10.1049/rpg2.12699

Venkateswari, R., & Rajasekar, N. (2021). Review on parameter estimation techniques of solar photovoltaic systems. In *International Transactions on Electrical Energy Systems* (Vol. 31, Issue 11). John Wiley and Sons Ltd. https://doi.org/10.1002/2050-7038.13113

Wang, Z., Liu, Y., Wang, R., & Hu, Y. (2024). Cost – Benefit Analysis of Cross-Regional Transmission of Renewable Electricity : A Chinese Case Study. *Sustainability*, *16*(10538), 1–21.

Xia, G., Draxl, C., Berg, L. K., & Cook, D. (2021). Quantifying the impacts of land surface modeling on hub-height wind speed under different soil conditions. *Monthly Weather Review*, *149*(9), 3101–3118. https://doi.org/10.1175/MWR-D-20-0363.1

Yimen, N., Hamandjoda, O., Meva'a, L., Ndzana, B., & Nganhou, J. (2018). Analyzing of a photovoltaic/wind/biogas/pumped-hydro off-grid hybrid system for rural electrification in Sub-Saharan Africa - Case study of Djoundé in Northern Cameroon. *Energies*, *11*(10), 1–30. https://doi.org/10.3390/en11102644

Zadehbagheri, M., Kiani, M. J., & Khandan, S. (2025). Designing a Robust SMC for Voltage and Power Control in Islanded Micro-grid and Simultaneous use of Load Shedding Method. *Journal of Operation and Automation in Power Engineering*, *13*(1), 74–87. https://doi.org/10.22098/joape.2023.12215.1910

Zulu, M. L. T., Carpanen, R. P., & Tiako, R. (2023). A Comprehensive Review: Study of Artificial Intelligence Optimization Technique Applications in a Hybrid Microgrid at Times of Fault Outbreaks. In *Energies* (Vol. 16, Issue 4, pp. 1–32). Multidisciplinary Digital Publishing Institute (MDPI). https://doi.org/10.3390/en16041786